analytical chemistry

Review

pubs.acs.org/ac

Micro Total Analysis Systems: Fundamental Advances and Applications

Damith E. W. Patabadige,[†] Shu Jia,[†] Jay Sibbitts,[†] Jalal Sadeghi,[†,‡] Kathleen Sellens,[†] and Christopher T. Culbertson*[,†]

[†]Department of Chemistry, Kansas State University, 213 CBC Building, Manhattan, Kansas 66506, United States

[‡]Laser & Plasma Research Institute, Shahid Beheshti University, Evin, Tehran, 1983963113, Iran

CONTENTS

It has been 14 years since the inaugural microfluidics review in *Analytical Chemistry* was published.[1] The first papers describing these devices which are also commonly referred to as Micro Total Analysis Systems, Lab-on-a-Chip (LOC), LabChips, microchips, or microfluidic devices generally focused on separations and the development of a variety of fluidic structures for sample manipulation and handling. The ultimate premise behind the development of these devices, however, has always been their potential to perform complete, automated chemical analyses as many of its monikers imply. Since the first review there has been remarkable progress in terms of developing truly sample-in/answer-out microfluidic devices that integrate multiple functional elements. Reports of novel individual components for these devices have now been surpassed by reports of devices with integrated functional elements that can actually perform partially automated or fully automated chemical analyses. There are, however, still some significant challenges facing the development of microfluidic systems especially in the areas of sample preparation, chip-to-real-world interfacing, and detection.

In terms of applications microfluidic devices have excelled in addressing a variety of biomedical analyses, especially those dealing with individual cells. This area has become so popular that it is now the subject of two additional *Analytical Chemistry* reviews, one on cellular analysis and the other on droplet microfluidics. There are, however, other application areas where the use microfluidic systems are popular, including drug screening, disease diagnosis, and nucleic acid analysis. In addition, the interest in developing clinical assays on paper microfluidic devices for use in resource poor situations has soared.

This review focuses on recent advances in microfluidic technology with an analytical focus in the areas of fundamental advances, integrated devices, and biomolecular assays since the last review published in 2014.[2] Reviews more tightly focused on cellular analysis and droplet microfluidics can be found elsewhere in this issue. We have tried to highlight some material, fabrication, coating, separation, and detection advances with more general applicability. We have not included, for the most part, papers on synthesis, biosensors, theory, simulations, or reviews. The papers included in this review were published between September 2013 and September 2015. The material was compiled using several strategies including

Special Issue: Fundamental and Applied Reviews in Analytical Chemistry 2016

Published: November 24, 2015

DOI: 10.1021/acs.analchem.5b04310
Anal. Chem. 2016, 88, 320−338

extensive searches using Scifinder, Web of Science, PubMed, and Google Scholar. The contents of high impact journals were also scanned, including *Analytical Chemistry*, *Lab-on-a-Chip*, *Nature*, *Proceedings of the National Academy of Sciences*, *Applied Physics Letters*, *Biosensors and Bioelectronics*, *Angewandte Chemie*, *NanoLetters*, *Science*, *Biomedical Microdevices*, *RSC Advances*, and *Langmuir*. More than 2500 papers relating to microfluidics were examined. We have attempted to identify some of the most interesting and promising papers for this review. We have grouped the papers into 4 main categories, fundamentals, functional elements, microfluidic platforms, and applications. Many papers, however, can fit into more than one category. Our category choice for each paper reflects the area in which we believed it made the most important contribution. Without a doubt we have missed a few excellent papers and had to eliminate others based on space constraints and readability. For those papers that we have failed to include, we apologize in advance and welcome comments regarding any oversight that we have made.

FUNDAMENTALS

Fabrication. *Materials and Bonding.* Polydimethylsiloxane (PDMS) remains the most common substrate material for microfluidic devices because of ease of fabrication, low cost, and transparency. Most of the devices reported in this review were fabricated with PDMS. However, when it comes to biological applications and mass production, other materials or surface modifications may be needed. Thermoplastics, for example, are attractive because they can be mass-produced via injection molding. For such materials, the hydrophilicity and ability to modify the channel surfaces is key, especially for biological applications. Recently modifications of cyclic olefin copolymer (COC) and poly(methyl methacrylate) (PMMA) microchip channel surfaces were studied using UV activation.[3] In this work, device channel aspect ratio and polymer type were found to be significant factors controlling surface activation. COC devices were found to be superior to PMMA devices for the creation of high-density active groups that could be used for surface modification.

Surface modifications can also affect chip bonding. Strong bonding is crucial in devices under high pressure. Covalent bonding using click chemistry between a molded thiol-ene-epoxy channel manifold and flat substrate was demonstrated[4] (Figure 1A). Because of the epoxy surface functionality, the channels in this device could also be modified easily to achieve spatially selective hydrophilicity control. A device fabricated from thio-acrylate resin was also reported.[5] Room temperature bonding between the two halves was achieved by fabricating one side with an excess of acrylate groups and the other side with an excess of thiol groups. Another method to enhance bonding between two surfaces is to use an adhesive. The adhesive has to be designed, however, so that it does not obstruct the channel manifold in the sealed device. To prevent potential channel clogging with adhesive, a UV curable glue, NOA81, was transferred to a glass substrate using a "spin and roll" tactic. This allowed the successful bonding of the glass to a fluorinated ethylene propylene (FEP film).[6] Nanoparticles were also shown to be a promising adhesive for elastic polymers where they can serve as a bridge between gel chains. Polydimethylacrylamide (PDMA) gel was reported to be glued by silica nanoparticles without heat or any other curing factors.[7] Although the bonding strength was only 1.6 J m^{-2},

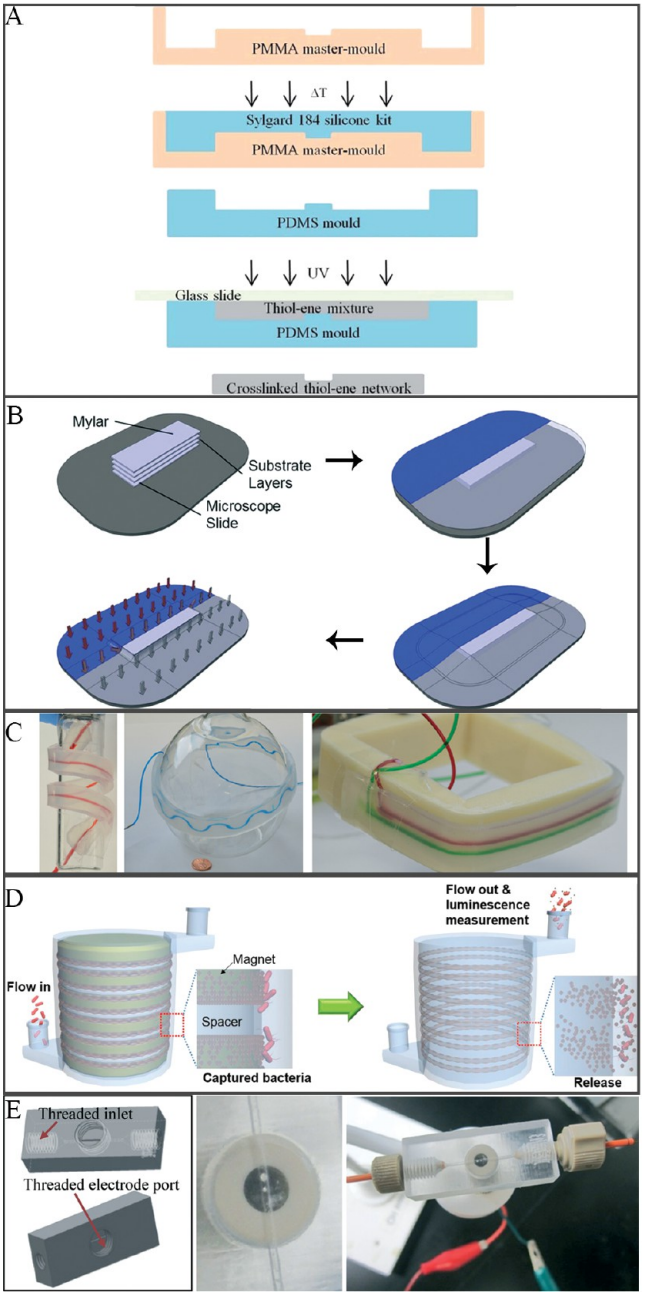

Figure 1. (A) Schematic of thiol-ene-epoxy chip fabrication. Reproduced from Mazurek, P.; Daugaard, A. E.; Skolimowski, M.; Hvilsted, S.; Skov, A. L. *RSC Adv.* **2015**, *5*, 15379−15386 (ref 4), with permission of The Royal Society of Chemistry. (B) Schematic of vacuum bag bonding. Adapted from Cassano, C. L.; Simon, A. J.; Liu, W.; Fredrickson, C.; Fan, Z. H. *Lab Chip* **2015**, *15*, 62−66 (ref 9), with permission of The Royal Society of Chemistry. (C) Reversible seal chips on complicated 3D structure. Adapted from Konda, A.; Taylor, J. M.; Stoller, M. A.; Morin, S. A. *Lab Chip* **2015**, *15*, 2009−2017 (ref 11), with permission of The Royal Society of Chemistry. (D) Schematic of 3D printed hollow magnetic capturing device. Reproduced from Lee, W.; Kwon, D.; Chung, B.; Jung, G. Y.; Au, A.; Folch, A.; Jeon, S. *Anal. Chem.* **2014**, *86*, 6683−6688. Copyright 2015 American Chemical Society. (E) 3D printed device with changeable electrode. Erkal, J. L.; Selimovic, A.; Gross, B. C.; Lockwood, S. Y.; Walton, E. L.; McNamara, S.; Martin, R. S.; Spence, D. M. *Lab Chip* **2014**, *14*, 2023−2032, with permission of of The Royal Society of Chemistry.

DOI: 10.1021/acs.analchem.5b04310
Anal. Chem. 2016, 88, 320−338

which was not competitive to that of heat or chemical bonding, nanoparticle gluing was simpler and more versatile.

As opposed to the chemical bonding approaches described above, heat embossing is one of the most popular ways to conduct thermoplastic bonding. A hybrid thermal technique was recently introduced to improve heat embossing.[8] In this process a high glass transition temperature (T_g) substrate was aligned, compressed and heated with an oxygen plasma treated low T_g cover plate. This bonding method is not limited to only thermoplastics as thermoplastic-silica substrates were also bonded in this manner. Another method reported to improve bonding utilized an "air bagging" technique. In this technique COC substrates were sealed in a vacuum bag that served to press the layers closely together evenly.[9] (Figure 1B) With a vacuum of ∼80 kPa, the COC's glass transition temperature was lowered. This allowed a lower bonding temperature and extended heating time without channel deformation. COC chips can also be bonded with ultrasound under a moderate amount of compression. However, with a conventional ultrasound setup, misalignment can occur due to polymer shrinkage and vibration during bonding. A self-balancing jig was developed to mitigate this problem.[10] The movable platform helped dispense vibrational energy keeping the relative positions of the two substrates stable.

Though irreversible bonding methods have been developed for stronger adhesion, reversible bonding is attractive for its flexibility and the potential to reuse substrates. PDMS devices are well-known for their reversible bonding capability. They can generate good seals on substrates with tens of micrometers roughness. To generate seals on substrates with larger roughness values external pressure must be applied to the PDMS. One recent study showed the potential to bond PDMS against rough complex surfaces using a combination of PDMS and Ecoflex.[11] Although it required a high pressure in the hundreds of kPa's to prevent any leakage, this highly elastic device can be placed on various 3D substrates instead of a flat substrate (Figure 1C). In another reversible bonding study, gecko-inspired dry adhesives were examined. The adhesive could sustain maximum pressures of 95 psi, whereas typical reversible PDMS bonding can only hold 5 psi at maximum.[12]

3D Printing. Since the last review period, 3D printing has emerged as a popular microchip fabrication method because of improvements in performance, printing resolution, speed, equipment availability, and costs.[13] With 3D printing, three-dimensional structures that are not accessible or not easily accessible using standard planar photolithography techniques can be fabricated. Stereolithography, as the earliest 3D printing method, was studied for low or medium volume commercial production.[14] Compared to standard planar photolithography and injection molding, 3D printing greatly reduces the cost of creating master molds and prototype chips. This expands access to commercial opportunities for many research or creativity based applications.

One example of a stereolithographically built microfluidic device used immunomagnetic nanoparticle clusters to enrich *Salmonella* bacteria from a large volume food sample (Figure 1D).[15] Dynamic mask projection stereolithography, another form of 3D printing, was used to fabricate microfluidic devices using a colorless resin with 60% light transmittance above 430 nm.[16] Mixers, gradient generators, and droplet generators were printed with typical channel dimensions of 200 μm in width and 30 μm in height. A complicated 3-layer chip was fabricated in 290 min for nitrate quantification. In another report, 3D printing was utilized to simulate cell culture by creating a blood vessel like channel with dimensions varying from 25 to 120 μm.[17] Water-soluble isomalt was used in heat projection to form a 3D sacrificial mold for soft media.[18]

While interfacing microfluidic devices to external devices is a difficult problem for many microchip fabrication methods, 3D printing can potentially provide easy solutions. For example a multimaterial 3D printed interconnect was applied and tested using pressures as high as 400 kPa.[19] With its outer positional parts, it can also be self-aligned. Another 3D printed monolithic microchip could host several threaded inlets intended for electrochemical detection.[20] (Figure 1E) Different microelectrodes were also coupled to the microchannel allowing multiple combinations electrochemical detection in the same channel.

Surface Modification. There is no one perfect channel surface chemistry. For this reason, the ability to modify a surface to suit a particular application is critical. Chemical modification can be used to alter a number of different surface properties including wettability, chemical stability/reactivity, and biocompatibility. For biochemical analysis, in particular, highly hydrophilic surfaces tend to reduce analyte nonspecific adsorption. Polyethylene glycol (PEG) is commonly used to modify surfaces to increase hydrophilicity. For example, the covalent attachment of PEG to a PDMS surface was achieved using a hydrosilylation reaction without changing the bulk PDMS modulus.[21] The modified surface contact angle decreased from 110° to 65°. Another PEG−PDMS device was fabricated following oxygen plasma treatment and silanization. This device had a reported shelf time as long as 28 days and good hemocompatibility.[22] While PEG remains the most popular choice to modify channel wall hydrophilicity, zwitterionic polymers, which have strong interactions with water, can also be applied via silanization.[23] Surface modifications for a variety of other microchip substrates have also been reported. For polycarbonate (PC) microfluidic substrates, a tunable hydrophilicity modification method was demonstrated based on aminosilane.[24] In addition to modifying hydrophobicity, the aminosilane coating was also used for bonding PC−PC devices. For PMMA-based centrifugal microfluidic discs, both poly(vinyl alcohol) (PVA) and (hydroxypropyl)methyl cellulose (HPMC) were spin-coated onto the discs to create a stable hydrophilic coating.[25] Finally hydrophilic modifications to PDMS, COC, PET, PC, and PTFE surfaces were performed via a simple dip and rinse silanization method. Using this method a copolymer of *N*-acryloyloxysuccinimide and glycidyl methacrylate could be attached and was able to stably decrease the water contact angle to around 50% of that of the original.[26]

In addition to changing the hydrophilicity of a surface, other surface modifications can be directed toward increasing the reactivity or interactivity of the surface to an analyte. Such surfaces can be used to concentrate or digest an analyte. Online enrichment of Hg^{2+} in water samples, for example, was realized by cross-linked gold nanoparticles in a microfluidic channel. Coupled to inductively coupled plasma mass spectrometry (ICPMS), this method achieved a LOD of 0.07 μg L^{-1}.[27] Alternatively on-chip digestion of double stranded DNA was carried out by an immobilized enzyme, λ-Exonuclease, using a 3-(3-(dimethylamino)propyl) carbodiimide/*N*-hydroxysuccinimide coupling.[28]

Coatings are often used to modify surfaces in microfluidic devices to improve separations. A recently reported CVD

DOI: 10.1021/acs.analchem.5b04310
Anal. Chem. 2016, 88, 320−338

process for coating aminosilanes onto a surface allowed electrophoretic separation of peptides with a separation efficiency of >600 000 and a peak capacity of 64 in <90 s.[29] This separation was directly interfaced with an ESI-MS for detection. A novel electrochromatography stationary phase was reported that used bovine serum albumin immobilized on a polydopamine/graphene supportive coating to form a sandwich structure for the chiral separation of D- and L-tryptophan.[30] These species were separated and quantified with LODs of 5.9 and 7.8 μmol/L, respectively.

FUNCTIONAL ELEMENTS

Fluid Control. *Acoustofluidics.* Recently acoustofluidics has increased in popularity due to its relative simplicity and versatility. Acoustofluidics employs the use of a piezoelectric component that is comprised of interdigitated transducers on a piezoelectric substrate. When an alternating electric field is applied, an acoustic wave is generated that propagates through the material in contact with the piezoelectric component. These acoustic waves are generally applied in two modes, namely, standing surface acoustic waves and traveling surface acoustic waves. Standing surface acoustic waves are generated when two surface acoustic waves interfere with each other creating regions of constructive and destructive interference that can be used to trap or sort particles. Traveling surface acoustic waves are generated by simply propagating an acoustic wave across a surface and allowing a portion of the acoustic wave to leak into the liquid which can generate mixing forces, streaming, and fluid translation (pumping).

One limitation to the use of acoustofluidics in microfluidic devices arises from the materials used in the piezoelectric transducer, namely, the piezoelectric substrate and the patterned electrodes. Popular bulk piezoelectric materials, such as quartz, are often brittle and difficult to integrate. As a result, interest in thin film piezoelectric materials has increased. An aluminum nitride film based piezoelectric transducer was recently developed.[31] Because the film was deposited onto a substrate instead of being cut from a bulk material, many transducer configurations are now available.[31] Besides the piezoelectric substrate, various electrode materials have been investigated. An electrode was fabricated from aluminum foil instead of the traditional patterned electrodes.[32] The foil was purchased from a grocery store and cut in the desired pattern using scissors. The use of this electrode material and fabrication technique eliminates the necessity of costly deposition equipment and clean room fabrication.

In addition to droplet microfluidics and particle manipulation, acoustofluidics can be used to pump fluids. Using acoustic waves to drive fluid flow is an attractive option, as it does not require external pneumatics or peripheral pumping equipment. A pumping pressure of 76 Pa was generated by the oscillation of tilted sharp-edge structures[33] (Figure 2A). Also, by using a pump design that directly interfaces the transducer with the fluid, high pumping efficiency and flow rates as high as 100 μL min^{-1} were generated.[34] Complex droplet manipulations, such as splitting and merging, were demonstrated by employing two piezoelectric transducers in a laterally offset configuration (Figure 2B).[35] Additionally, nanoliter scale fluid mixing was performed using ultrahigh-frequency surface acoustic waves to induce acoustic streaming.[36]

Another area explored by acoustofluidics is the manipulation and sorting of both particles and cells. For cytometry, cells or particles can be directed to a desired region within a channel for

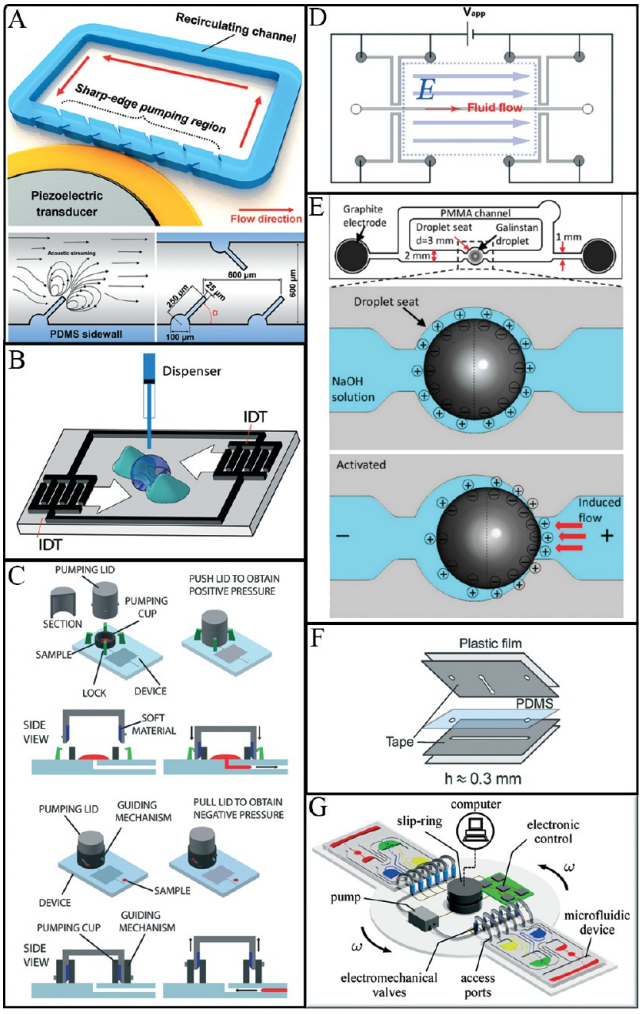

Figure 2. (A) Schematic of the tilted sharp-edge-based device. Adapted from Huang, P.-H.; Nama, N.; Mao, Z.; Li, P.; Rufo, J.; Chen, Y.; Xie, Y.; Wei, C.-H.; Wang, L.; Huang, T. J. *Lab Chip* **2014**, *14*, 4319 (ref 33), with permission from The Royal Society of Chemistry. (B) Schematic of laterally offset piezoelectric transducers. Adapted from Collignon, S.; Friend, J.; Yeo, L. *Lab Chip* **2015**, *15*, 1942 (ref 35), with permission from The Royal Society of Chemistry. (C) Schematic of the method to generate positive pressure (left). Schematic of the method to generate negative pressure (right). Adapted from Begolo, S.; Zhukov, D. V.; Selck, D. A.; Li, L.; Ismagilov, R. F. *Lab Chip* **2014**, *14*, 4616 (ref 43), with permission from The Royal Society of Chemistry. (D) Schematic of liquid metal enabled electroosmotic pump. Adapted from Gao, M.; Gui, L. *Lab Chip* **2014**, *14*, 1866 (ref 44), with permission from The Royal Society of Chemistry. (E) Schematic of liquid galinstan droplet enabled pump. Adapted Tang, S.-Y.; Khoshmanesh, K.; Sivan, V.; Petersen, P.; O'Mullane, A. P.; Abbott, D.; Mitchell, A.; Kalantar-zadeh, K. *Proc. Natl. Acad. Sci. U.S.A* **2014**, *111*, 3304 (ref 46), with permission from National Academy of Sciences. (F) Schematic of thin multilayer valve fabrication. Adapted from Cooksey, G. A.; Atencia, J. *Lab Chip* **2014**, *14*, 1665 (ref 47), with permission from The Royal Society of Chemistry. (G) Schematic of the integrated active pneumatic control system. Adapted from Clime, L.; Brassard, D.; Geissler, M.; Veres, T. *Lab Chip* **2015**, *15*, 2400 (ref 156), with permission from The Royal Society of Chemistry.

downstream detection.[37] Using acoustic waves for manipulation and separation offers the ability to perform contactless and label free sorting. Size-based separations of particles have been developed with reported resolutions below 1 μm.[38,39] Acoustic

DOI: 10.1021/acs.analchem.5b04310
Anal. Chem. 2016, 88, 320−338

methods of separating cells based upon their physical properties have also been reported.[40] Using acoustics for cell separations offers many advantages over traditional methods due to biocompatibility that arises from the contactless and non-destructive nature of acoustofluidics. Rare circulating tumor cells were separated from peripheral blood and were still viable postseparation. Keeping the cells intact and viable allowed further analysis of these rare cells to be conducted, which enabled improved diagnostic capabilities and assessment of the efficacy of cancer treatments.[41,42]

Active Pumping. The generation of fluid flow in microfluidic devices has always been a challenging obstacle. External pressure sources are often difficult to integrate and increase the footprint of any microfluidic system that employs them. As a result, the elimination of external pressure sources has been a driving force in the development for novel pumping devices. One such innovation utilizes a simple component, called a pumping lid, which fits onto a device and allows for controlled generation of pressure.[43] Operation of the pumping lid is as simple as pushing a button (Figure 2C). The lid is placed at the desired reservoir and once the user pushes down on the lid a positive pressure is generated. Negative pressure can also be generated by performing the opposite action and pulling up on the lid.

Although pressure driven pumping is the most straightforward pumping mechanism, electric field driven pumps have also been investigated. One challenge that arises when developing electric field enabled pumps is the electrode required. Patterned electrodes require expensive equipment and are often fragile. As an alternative to solid electrodes, liquid metal electrodes have received some attention. An electroosmotic pumping device that used liquid metal electrodes was developed.[44] The liquid metal electrodes occupied channels adjacent to the fluidic channel (Figure 2D). When a potential was applied between the upstream and downstream electrodes, an electric field and subsequently electroosmotic flow was generated. One key advantage to this configuration was the absence of contact between the fluidic channel and the electrodes. This eliminated the possibility of undesired electrochemical reactions on the electrodes. Another group has developed a device operating on a similar principle but employed the use of a salt water solution in lieu of liquid metal to generate an electric field.[45] Additionally, a liquid metal enabled pump was developed by placing a drop of liquid metal, galinstan, in a confined portion of a channel[46] (Figure 2E). An alternating voltage was then applied, causing the surface charge of the drop to redistribute resulting in a shift of the drop and the displacement of liquid.

Valves. Valves created using multilayer lithography first introduced by the Quake group are extremely popular and have inspired many derivative approaches to creating valves and pumps in microfluidic devices. By varying the geometry and configuration of the control and fluidic channels in these multiplayer chips, pneumatically controlled membrane valves have taken on a variety of forms. A new fabrication technique was developed that utilized the traditional geometry of the Quake valve but alters the assembly.[47] The valve membrane was still fabricated from PDMS; however, the channels were made by cutting a pattern into a plastic laminate and folding the two layers onto each other with the membrane sandwiched in between (Figure 2F). The use of thin plastic films allow for devices to consist of several layers without appreciably increasing the thickness, as is the case in traditional fabrication methods. Pneumatically actuated membranes have also been adapted to serve other purposes such as pressure regulation.[48] A passive flow regulator was developed with reported flow rate ranges exceeding its predecessors. Additionally, a particle trapping device was reported that was capable of 100% loading and trapping efficiency.[49] A series of pneumatic valves was used to selectively trap and release beads of interest, which could be applied to high-throughput screening methods. A device featuring vacuum controlled actuating chambers was also developed.[50] This allowed the controlled activation of one cell population and the isolation of an adjacent one. In another device applied to cellular analysis, a clogging free device was developed.[51] This particular valve configuration allowed the user to expand the fluidic channel to dislodge any cell aggregates.

While there has been much interest in exploring pneumatically controlled valves, other valve options have also been investigated. Liquid based gating valves are one example. Gating valves operate based upon the principle of capillary pressure. In a centrifugal microfluidic devices, varying spinning speeds were used to control when the centrifugal force exceeded the liquid's capillary force to cause the desired fluid flow.[52] The geometry used in this gating valve allowed for the control of flow direction without changing the direction of rotation. In another microfluidic device, a gating liquid was used to fill a pore to act as a barrier.[53] Once the pressure of the transporting substance (liquid or gas) exceeded the capillary force within the pore, the gating liquid would part allowing the passage of the transporting substance. Once the pressure was released, the gating liquid would refill the pore, restoring the barrier. The gating liquid had a higher affinity for the pore material than it did for the transporting substance, thus minimizing the potential for fouling.

Gradient Formation. The laminar flow characteristics found in microfluidic channels allows for temporally and spatially stable gradients to be generated. These gradients can used in a variety of applications from chemotaxis to toxicity testing and drug screening. Recently a gradient of antibiotic was generated in an agarose film between a source and sink channel.[54] Culturing cells on this film allowed an antibiotic's inhibitory ability to be examined easily in real time. In order to establish a uniform flow over a large area in a channel, for example, a biofilm, a large chamber instead of a flow channel was fabricated.[55] Under such continuous gradient, the effects of nutrients and toxic substances on biofilm growth were better observed.

Mixing. Because of the low Reynolds number laminar flow in microchannels, mixing generally takes place due to molecular diffusion and, therefore, is slow. To improve passive mixing, special geometries are often employed that require no external energy input. An alternative to passive mixing was recently reported that used a vortex generated from nonequilibrium electrokinetics within a channel filled with assembled nanoparticles.[56] The 3D assembled nanoparticles provided one more dimension to enhance mixing performance. The 2-fold shorter mixing times and a 30 4-fold shorter mixing length were achieved compared to 2D microchannels. A U-turn turbulence generator was able to mix streams in 5.5 μs.[57] With such a fast mixing ability, a DNA hairpin intermediate could be observed in G-quadruplex formation.

Analyte Concentration. The ability to concentrate analyte that is present at low concentrations can be very important, especially when working with biological samples. Recently, detection of rare cellular species has proven to be a viable

DOI: 10.1021/acs.analchem.5b04310
Anal. Chem. 2016, 88, 320−338

method for diagnoses of various diseases. One of the major hurdles, however, is their extremely low abundance. As a result, preconcentration of these cells has been the focus of many studies. A recent report used functionalized magnetic beads to capture, isolate, and retrieve rare species. One group developed a method that used beads functionalized with pathogen binding ligands to isolate and detect pathogen cells at concentrations below 1 cell per milliliter of human blood.[58] Magnetic beads have also been used to isolate specific bacteria from cell cultures.[59] By embedding permanent micromagnets within a microfluidic channel, magnetically labeled bacteria were successfully isolated from a larger cell population. Multiplexed detection of low concentration cancer biomarker proteins have also been realized with the aid of magnetic beads.[60] Magnetic beads derivatized with enzyme labels and antibodies were used to capture target proteins which were then detected downstream amperometrically. Magnetic analyte preconcentration has also made its way into centrifugal microfluidics. A device that isolates cells that are selectively labeled based on phenotype was reported.[61] Spiked whole blood samples were spun, causing unlabeled cells to move radially and labeled cells to be deflected into a separate reservoir for fluorescence quantification. Other mechanisms of sample preconcentration have been reported. A device combining inertial microfluidics and steric hindrance was able to sort and preconcentrate cells on the basis of size and deformability.[62] The separation required no labeling of cells and had a reported throughput exceeding 20 million cells/min. Another group utilized a 3D nest-like network decorated with gold nanoparticles to adsorb bovine serum albumin in the picomolar range.[63] Preconcentration methods have also been applied to nanoparticle-based probes. Gold nanoparticles were functionalized with fluorescently labeled dog serum albumin and preconcentrated by the application of an electric field.[64] The fluorescence of the dye was quenched by the gold nanoparticles. The probes were used to perform an activity assay of a protease. Upon cleavage of the dog serum albumin, the quenching of the fluorescent probe would cease and an increase in fluorescent signal would be observed.

Separations. Reports of novel separation modalities have decreased significantly as most standard conventional separation techniques have been integrated onto microfluidic devices. In addition, the development of novel separation techniques that take advantage of either microchip fabrication methods or novel microfluidic channel geometries has also slowed. In many ways this area of microfluidic technology has matured. There were still, however, a limited number of novel separation approaches that have recently been reported focusing on particle (including cell) size differentiation. The fabrication of devices for sieving or size-based separations can be challenging because of the general complexities involved in the process. There have, however, been some novel systems reported including a device focused on the separation (filtration) of macromolecules (e.g., single stranded DNA and IgG) from larger particles using *in situ* fabricated membranes. In this approach horizontally oriented 10 μm thick silicon membranes were fabricated inside a 20 μm deep microchannel. Controlled size pores were grown between membranes along the lateral direction. Using this membrane filter, 300 nm diameter polymer beads were successfully retained behind the membrane while macromolecules permeated it.[65] In another report, size differentiation of particles was demonstrated based on their lateral equilibrium positions.[66] The ability to separate particles based upon their size arose from the shape of the channels. As differently sized particles were pumped around turns (or corners) in channels, the particles moved into separate flow paths based on their inertia. Mixtures containing florescent microbeads (3−13 μm) were separated by driving them through a 200 μm wide square wave shaped microchannel. Separation purities greater than 90% were achieved depending upon on the nature of the mixtures (Figure 3A).[66]

While most charged particles are separated using electrophoresis, some may also be separated using magnetic fields.

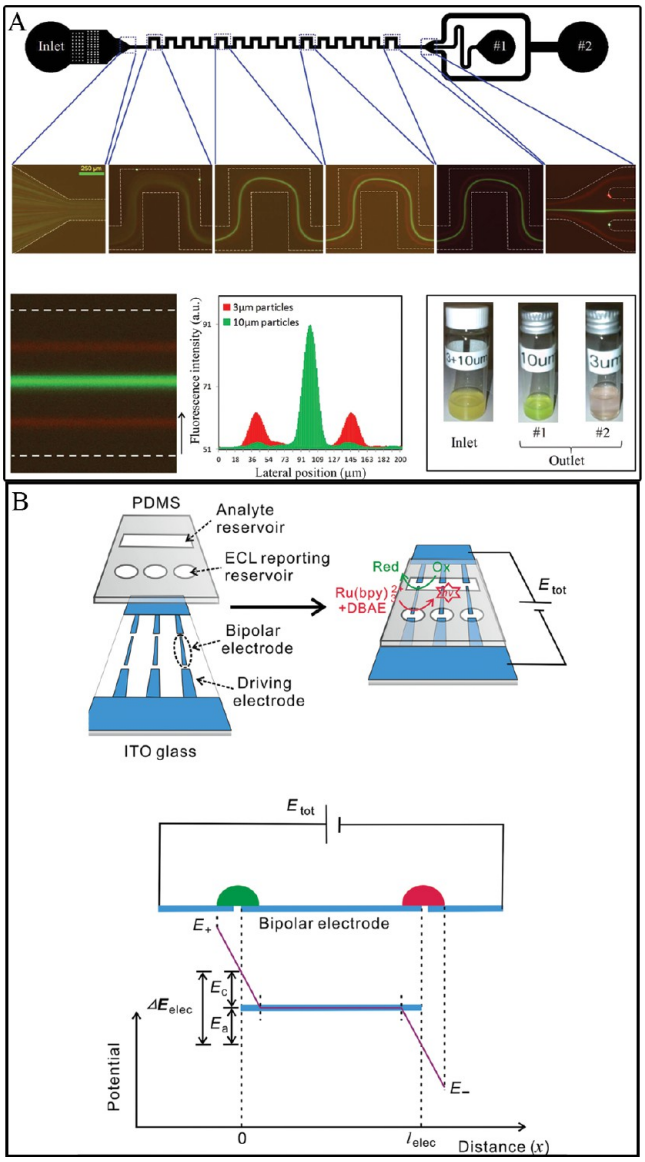

Figure 3. (A) Schematic illustration of microfluidic system used to separate mixtures of microbeads. Separation principle is based on inertia of the particles. Reproduced from Zhang, J.; Yan, S.; Sluyter, R.; Li, W.; Alici, G.; Nam-Trung, N. *Scientific Reports* **2014**, *4*, 4527 (ref 66). Copyright 2015 The Nature Publishing Group. (B) Schematic of microdroplet based bipolar ECL imaging. PDMS layer is integrated with glass substrate that composed of series of paralel bipolar ITO electrodes. Reprinted from *Biosens. Bioelectron.*,Vol. 53, Wu, S.; Zhou, Z.; Xu, L.; Su, B.; Fang, Q. Integrating bipolar electrochemistry and electrochemiluminescence imaging with microdroplets for chemical analysis, pp. 148−153 (ref 77). Copyright 2015, with the permission from Elsevier.

DOI: 10.1021/acs.analchem.5b04310
Anal. Chem. 2016, 88, 320−338

Recently a Y shaped microchannel was used to separate charged particles based upon their interaction with a magnetic field.[67] The microchannels were filled with suspensions of magnetic nanoparticles (ferrofluids) and an external magnetic field was used to separate oppositely charged particles by magnetophoresis. The magnetic field altered the trajectories of the particles thus allowing a separation into different forks of the Y channel.

In many clinical applications cell separations are critical. This includes the high throughput and accurate separation (isolation) of circulating tumor cells (CTC). During the past decade, microfluidic systems developed for sorting applications have provided throughputs in the range of 1−3 kHz. Recent advancements in microfluidic cell sorting systems have pushed these throughputs up to 30 kHz.[68] Such throughputs were achieved by integrating a gap divider into a microchannel instead of impermeable membranes that have been utilized in most other previously reported techniques. This technique provides >99% accuracy with electric field guided droplet control. The throughput for these devices, however, is still lower than for commercially available (50 kHz) cell sorters, and this technique may not be useful with nonfluorescent sorting applications.

Detection. The usefulness of microfluidics for chemical analysis applications is largely dependent upon the types for detectors that can be integrated with the fluidic manifold or coupled to it. For many applications, it is desirable to integrate a detector without significantly increasing the overall device footprint, cost or complexity. Many miniaturized detection techniques have been demonstrated and additional ones are still being introduced in order to improve key detection features including sensitivity, selectivity, and limit of detection (LOD).

Electrochemical. Among detection techniques, electrochemical approaches are especially interesting because of the compatibility with micro/nanofluidics, ease of integration, and the ability to perform a variety of electrode modifications to improve sensitivity, selectivity, LOD, resolution, separation efficiency, and reproducibility.[69] For example, carbon fiber microelectrodes embedded in PDMS and pyrolyzed photoresist film electrodes (PPF) fabricated on glass substrates were characterized using the electrophoretic separation of dopamine metabolites followed by amperometric detection.[69] In addition to amperometry, voltammetry and even the combination of both techniques[70] are popular to integrate into microfluidic devices. For example, the feasibility of using pencil lead (graphite) to draw electrodes on paper based microfluidic devices was recently reported.[71,72] In this approach, electrode characterization was performed via voltammetry with reproducible results.[71] In addition, a 15 cm long pencil lead was used to draw thousands of electrodes resulting in better precision for voltammetric studies of decamethylferrocene (i.e., RSD % are 4% and 2% for peak height and peak potential, respectively). However, some electrode microfabrication techniques still face challenges as electrodes may spontaneously form "lift-off ears" (sharp metal edges). Lift-off ears are problematic since sharp edges generate strong electric fields and interfere with the reproducibility of results. A novel approach successfully addressed this issue by introducing an additional etching step during the electrode fabrication process which was followed by the deposition of a 500 nm silicon nitride protective layer to improve the electrode stability without compromising performance.[73] In order to characterize the microfluidic system with 12 individual integrated electrode sites, DNA hybridization events and glucose sensing were demonstrated using impedance spectroscopy and cyclic voltammetry (CV), respectively.[73] In another application, a PDMS-based microfluidic device composed of a simple straight channel was integrated with an electrode printed platform in order to perform anodic stripping voltammetry. CDSe@Zns quantum dots (QD's) were used as carriers of apploliprotein E (biomarker for Alzheimer's disease), and the electrochemical response of cadmium was used to quantify the biomarker.[74]

Many biosensing approaches that are integrated in microfluidic devices are based on electrochemical detection including a couple of recent papers that focused on measuring the activity of glucose oxidases (GOx) using nanowires[75] and miniaturized electrodes.[76] For example, a paper based 3D origami electrochemical device that was composed of Au nanoparticles and MnO_2 nanowires was used to monitor such activity.[75] Another approach demonstrated the ability of using droplet based microfluidic devices integrated with Pt black microband electrodes to enhance GOx detection sensitivity by ∼10-fold compared to a Pt microband electrode.[76]

Electrochemically induced chemiluminescence (ECL) is another electrochemical technique that has been used in a variety of microfluidic devices for bioanalytical applications. Compared to fluorescent techniques, these detection methods do not require an external light source or additional instrumentation. Hence, noise produced by scattered light can be significantly minimized. Most often ECL detection is performed using bipolar microband electrodes (BPE) that are fabricated on indium tin oxide (ITO) coated glasses. Current generated by cathodic and anodic reactions at the two poles of the BPE drive chemiluminescence at the anodic pole (Figure 3B).[77] This phenomenon has been recently utilized for the detection of cancer biomarkers using a multichannel microdroplet-based microfluidic device composed of an array of BPEs.[78] The electrodes in these types of devices have the ability to both drive ECL reactions for imaging and to serve as electrochemical (amperometric and voltammetric) detectors.[77]

Optical Detection. Many conventional optical detection methods can be and have been integrated with microfluidic devices including fluorescence, chemiluminescence, scattering, diffraction grating, plasmon resonance (PR), and surface-enhanced Raman spectroscopy (SERS).[79,80] Optical detection can oftentimes be enhanced through the integration of chemically and biologically active structures fabricated within the channel manifold. These structures may be larger or smaller than the biological targets of interest. Recently a highly sensitive fluorescence detector was reported based on the miniaturization of a supercritical angle fluorescence (SAF) array. To increase throughput, the truncated cone-shaped SAF was fabricated to collect light at a large collection angle to enhance the fluorescence signal ∼46× higher than that of a conventional microscope.[81] A photonic crystal (PC) microchip consisting of a novel dielectric material was used for the ultratrace detection of fluorescence analytes. This device was fabricated by inkjet printing and capable of ultratrace detection down to 10^{-16} mol L^{-1}.[82] Fluorescence-based pathogen detection was also carried out with a thiol−acrylate microfluidic device prepared via soft lithography.[5] In this method, nonspecific binding of lipopolysaccharides (LPS) to the microfluidic walls was blocked using casein which reduced the background fluorescence of the substrate ∼14 times. This thiol−acrylate device was able to detect *E. coli* O55:B5 LPS down to 1 μg mL^{-1} and *E. coli* O157:H7 down to 10^5 cfu mL^{-1}.

DOI: 10.1021/acs.analchem.5b04310
Anal. Chem. 2016, 88, 320−338

Although excitation sources, microscopes, charge-coupled devices (CCDs), and photomultiplier tubes (PMTs) can be integrated with microfluidic devices with good detection limits, often they cannot be used for high-throughput excitation, observation, and detection due to their bulky volumes. Recently, some miniaturized devices have been demonstrated that enhance these properties. For example, an optofluidic complementary metal-oxide-semiconductor (CMOS) platform (Figure 4A) was described as a simple method for the ultrahigh-throughput parallel interrogation of drops. This device was consisted of 16 parallel microfluidic channels (Figure 4A) bonded directly to a CMOS sensor array that collected fluorescence signals emitted from the drops. Counting capability exceeded 254 000 drops/s.[83] Another interesting miniaturized optical multicolor fluorescence detector reported was an inexpensive (~$9US) mini-microscope fabricated from a webcam and off-the-shelf components[84] (Figure 4B). This detector was able to temporally monitor cell migration and analyze the beating of microfluidic liver and cardiac bioreactors in real time, respectively. It had adjustable magnification from 8× to 60× and achieved a lateral spatial resolution of <2 μm.

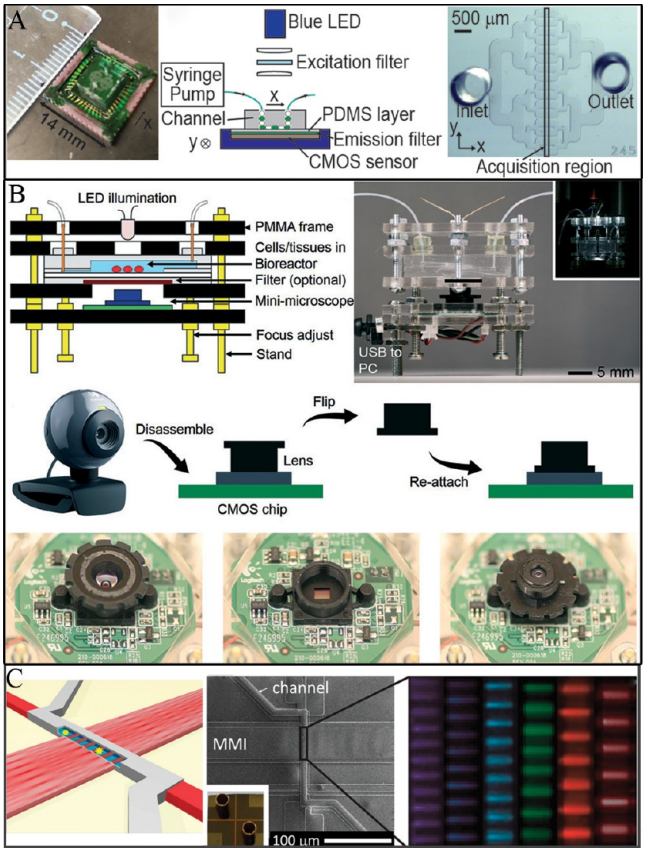

Figure 4. (A) Photograph and experimental setup of the device consisting of a microchannel bonded directly on a CMOS sensor. Reproduced from Kim, M.; Pan, M.; Gai, Y.; Pang, S.; Han, C.; Yang, C.; Tang, S. K. Y. *Lab Chip* **2015**, *15*, 1417−1423 (ref 83), with permission of The Royal Society of Chemistry. (B) Schematic and photograph showing the design of the mini-microscope integrated with a bioreactor and fabrication of the imaging unit. Reproduced from Zhang, Y. S.; Ribas, J.; Nadhman, A.; Aleman, J.; Selimovic, S.; Lesher-Perez, S. C.; Wang, T.; Manoharan, V.; Shin, S.R.; Damilano, A.; Annabi, N.; Dokmeci, M. R.; Takayama, S.; Khademhosseini, A. *Lab Chip* **2015**, *15*, 3661−3669 (ref 84), with permission of The Royal Society of Chemistry. (C) Schematic view of MMI waveguide, scanning electron micrograph of MMI-based optofluidic chip and photographs of multispot excitation patterns, respectively, from left to right. Reproduced from Ozcelik, D.; Parks, J. W.; Wall, T. A.; Stott, M. A.; Cai, H.; Parks, J. W.; Hawkins, A. R.; Schmidt, H. *Proc. Natl. Acad. Sci. 112*, 12933−12937 (ref 85). Copyright 2015 United States National Academy of Sciences.

Many micro-optofluidics devices are used for the detection, manipulation, and analysis (cytometry) of cells.[85,86] The ability to simultaneously detect and identify multiple biomarkers or biological particles is a key requirement for molecular diagnostic tests. To meet this requirement, recent microfluidic systems have been reported that use multiplexed micro-optofluidic platforms. For example, the detection of three individual fluorescently labeled influenza A subtypes was demonstrated using a single multimode interference (MMI) waveguide.[85] In the MMI, because of the interference of multiple modes with each other, separated spots were created at the liquid-core waveguide section (Figure 4C). These signals were produced by creating color-dependent excitation spot patterns from a single integrated waveguide structure (Figure 4C). In a second system, airborne *Escherichia coli*, *Bacillus subtilis*, and *Staphylococcus epidermidis* cells were hydrodynamically focused at an intersection and then detected via fluorescence and scattering using optical fibers integrated into the micro-optofluidic platform. This device reduced the analysis time of airborne microorganisms with improved accuracy compared to conventional microorganism-counting methods.[86] A third integrated device was used to detect single λ-DNA molecules both electrically and optically on a nanopore-gated opto-fluidic chip. Single molecule sensitivity with absolute flow velocity was verified by using correlated optical and electrical signals.[87]

Parallel with opto-microfluidic cytometry new cell imaging developments were reported for single cells, organelles and specific macromolecules.[88] One novel single cell imaging approach used a mathematical algorithm to analyze spatial-temporal data obtained from fluorescence and scattering signals. Uniquely two PMT detectors were used, instead of CCDs or fast cameras, to create high quality images of moving cells. The design could be incorporated into microfluidic flow cytometers to generate cell imaging.[89]

Recently, advances in the field of nanophotonics combined with fluorescence have increased its popularity for single molecule detection in microfluidic systems.[90,91] This single-molecule sensitivity requires overcoming the diffraction-limited optics[90] of confocal techniques which are restricted to concentrations in the pico to nanomolar range in femtoliter detection volumes.[92] The transient interaction between enzymes, proteins, and nucleic acids, however, occur at micromolar concentrations; therefore, single molecule detection of such interactions requires a reduction in the detection volume over 3 orders of magnitude below that typically used.[92,93] This was achieved using plasmonic nanoantennas to enhance the luminescence of quantum emitters.[94] For example, a double nanohole (DNH) structure was milled into a metal film which provided fluorescence enhancement up to several hundred fold while the detection volume was confined in a range below 100 zeptoliter (1 zL = 10^{-21} L). Zero-mode-waveguides (ZMW) consisting of nanoapertures on metallic substrates were used to image a large number of single molecules in live cell experiments.[95] Finally an aptamer−carboxyfluorescein/graphene oxide energy transfer system was

DOI: 10.1021/acs.analchem.5b04310
Anal. Chem. 2016, 88, 320−338

used to detect proteins in complex solutions without the need for pretreatment[96]

Surface Plasmon Resonance (SPR). SPR techniques can be integrated with microfluidic devices for the detection of macromolecules on adsorbed surfaces. Detection sensitivity can be enhanced by reducing the distance between metallic films utilized in such detectors and the analytes. Many novel approaches already have focused on developing Ag, Au, and SiO_2 nanoparticles to improve the sensitivity. More recent work has focused on using concentrated core−shell-Ag@SiO_2 nanoparticles in micro/nanochannel devices in order to detect oxidative species that are released in cigarette smoke with SPR-enhanced fluorescent detection.[97] This was further extended to localized surface plasmon resonance technology (LSPR).[98] The LSPR detector was integrated into a PDMS/glass hybrid device where pneumatically controlled microvalves were used to perform automated fluid handling (Figure 5A). Excellent detection limits were achieved due to Au nanorods assembled on the glass substrate. In order to monitor cancer biomarkers in human blood serum, eight microchannels consisting of 30 two individually monitoring sites were used.[98] Such label-free and highly reproducible biosensing techniques might be well suited to clinical applications. The complexity and bulkiness of the setup, however, are drawbacks of these systems. In order to make SPR easier to implement, a highly sensitive biochip for label-free detection of imidacloprid pesticides was combined with a simple portable imaging setup (Figure 5B).[99] The sensing part consisted of several nanoslit arrays, which made a spectral image on a chip from the distribution of transmitted lights. Qualitative and semiquantitative analyses of pesticides were directly observed from spot shifts of analyte by the eye or a smartphone. This visual SPR approach with LODs as low as 1 ppb was well below the maximum residue concentration permitted by law (20 ppb).

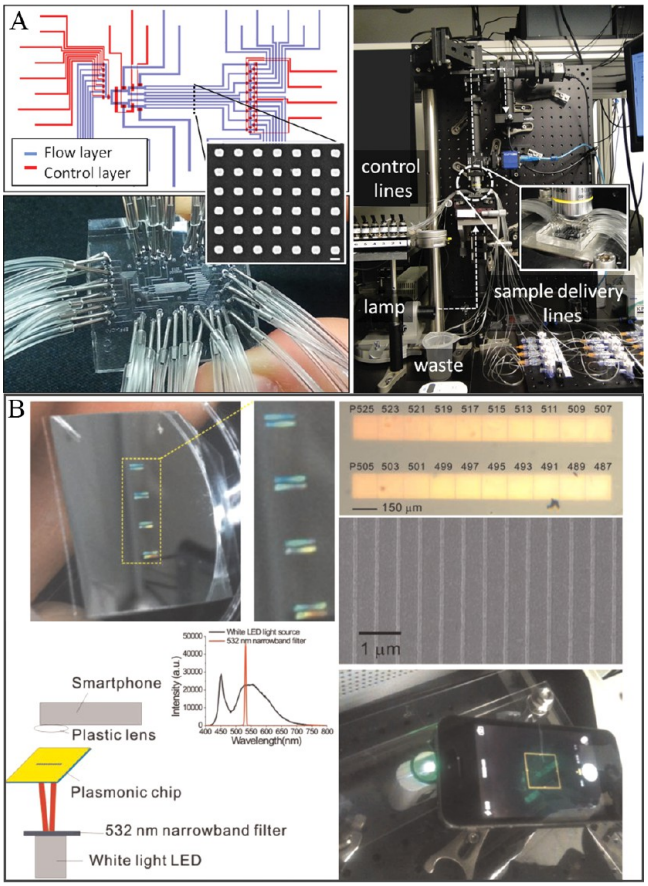

Figure 5. (A) Overview of microfluidic sensing system, schematic of integration of microfluidic channels with pneumatic control channels and SEM image (scale bar = 200 nm) of orientation of plasmonic gold nanorods. Reproduced from Acimovic, S. S.; Ortega, M. A.; Sanz, V.; Berthelot, J.; Garcia-Cordero, J. L.; Renger, J.; Maerkl, S. J.; Kreuzer, M. P.; Quidant, R. *Nano Lett.* **2014**, *14*, 2636−2641 (ref 98). Copyright 2014 American Chemical Society. (B) Optical image of the plasmonic biochip using a smartphone. Reprinted from *Biosens. Bioelectron.*,Vol. 75, Lee, K.L.; You, M.L.; Tsai, C.H.; Lin, E.H.; Hsieh, S.Y.; Ho, M.H.; Hsu, J.C.; Wei, P. K. Nanoplasmonic biochips for rapid label-free detection of imidacloprid pesticides with a smartphone, pp. 88−95 (ref 99). Copyright 2015, with the permission from Elsevier.

Surface Enhanced Raman Scattering (SERS). With the discovery of Raman signal enhancement on roughened silver surface by Martin Fleischmann and co-workers in 1974, much work has been focused on this field.[100] Recently more SERS detectors have been integrated into microfluidic devices because of their strong potential for nondestructive, label-free, and highly sensitive real time detection.[101] This has opened up new possibilities for high-throughput detection of organic reactions at the micro/nanoscale.[102] In SERS, to provide sensitive detection, the analyte has to be within close proximity of the immobilized metal film or nanostructure on the substrate. However, having analytes in the solution phase causes a significant reduction in detection sensitivity due to molecular diffusion. One way of addressing this issue is using sheath flow[103] or hydrodynamic focusing in confined microfluidic channels over the SERS active electrode. If the analytes are electrically active, dual detection can be performed via both amperometric detection and SERS detection.[104] On the other hand increasing the surface area of the immobilized metal surface can increase analyte interactions dramatically. Using nanoporous gold disks (NPGD) as a Raman enhancing surface, increasing the nanostructured surface area was shown to increase the signal ~20-fold compared to the existing techniques.[105] Another report used NPGDs for label-free monitoring of ssDNA hybridization events (with LOD 20 pM) without reducing the performance of the detection system.[106] Finally, a novel nanoarchitecture using polymer nanoassembled particles as a SERS substrate in microfluidic devices was used for simultaneous fluorescence, LSPR, and SERS detection.[107]

Mass Spectrometry. Mass spectrometry (MS) is a powerful tool for the detection of analytes with high specificity and high sensitivity. Microchip electrophoresis (ME) coupled with electrospray ionization (ESI) provides great advantages in terms of fast analysis and higher peak capacity compared to ultraperformance liquid chromatography (UPLC) separations coupled with MS. This is especially true in hydrogen exchange mass spectrometry (HX-MS), which requires rapid analysis to recover deuterium.[108] Furthermore, the integration of a series of microband electrodes within a microfluidic device allowed the production of rapid electrochemical responses for metabolites formed during drug oxidation. A recent report demonstrated that the lag time between the oxidation process and mass analysis was significantly reduced using a microfluidic-ESI-MS device.[109] Also, the microfluidic analysis of metabolites through isoelectric focusing techniques has been coupled with matrix-asssisted laser desorption ionization-time-of-flight mass spectrometry (MALDI-TOF MS).[110] This technique, however,

DOI: 10.1021/acs.analchem.5b04310
Anal. Chem. 2016, 88, 320−338

was less efficient compared to the time scale of the previously described system since it involved device deassembly and sample freezing after separation and before introduction into the mass analyzer.[110] Droplet based microfluidic systems have also been recently used with inductively coupled plasma mass spectrometry (ICPMS). In this device red blood cells were incorporated into highly volatile perfluorohaxane droplets in order to introduce them into the ICPMS system. Such droplets were introduced into the system with <50% efficiency thereby reducing the throughput of the device significantly. The bulkiness and complexity of the system may limit microfluidic applications.[111]

Impedance. Impedance detection became popular for bioanalytical applications a couple of decades ago, especially in flow cytometry associated with microfluidics. This is a label-free,[112,113] nondestructive[112−114] alternative to flow cytometry with laser-induced fluorescent detection (LIF). Trapping particles/single cells in the microchannels allows the measurement of impedance in the presence of an ac current and voltage across the microchannels. In most cases, patterning gold electrodes for such detectors is expensive; hence, building low cost sensors is challenging. In order to reduce the cost and increase the reusability, electrodes were fabricated on a printed circuit board (commercially available at the cost of ~$2.00 per circuit) and integrated with a microfluidic channel manifold.[113] Similar sensors were used to detect bacterial nucleoid structures[112] and bacteria in drinking water with LODs as low as 10 cells/mL via a smartphone app.[114]

Conductivity. Conductivity is a universal detection technique that has recently been implemented to characterize tumor cells in miniaturized fluidic systems. This new approach characterized tumor cells based on electrical properties such as membrane capacitance and cytoplasm conductivity.[115] Although, electrolyte conductivity (EC) sensors are common, issues with bubble nucleation, surface fouling, and low durability are often encountered. Recently these were addressed using a capacitively coupled contactless conductivity detection (C^4D). However, this detector has poorer LODs than in channel conductivity detectors because of the additional impedance introduced by surface coating. To improve detection limits, a highly conductive protective layer composed of perovskite oxide of barium strontium titanate (BST) was used and demonstrated similar performance compared to EC sensors.[116] Most microsensors are limited to 2D planar structures in microfluidic devices due to fabrication and channel integration issues. To partially overcome this limitation, tubular 3D microsensors (Figure 6A) have been reported that provide a 2-fold sensitivity enhancement compared to 2D sensors with poorer LODs.[117]

Other. Recent studies demonstrated the possibility of using silicon/quartz hybrid microreactors for studying the *in situ* crystal formation of $CaCO_3$.[118] Furthermore, it was shown that both small-angle X-ray scattering (SAXS) and wide-angle X-ray scattering (WAXS) techniques could be used to monitor the on-chip crystallization of rhombohedral calcite and study the characteristic properties of the crystals.[118] In addition, the nuclear magnetic resonance (NMR) technique has been extended to many microfluidic applications including high spatial resolution detection.[119] A recent report demonstrated the possibility of using μNMR as a clinically applicable method to detect lung cancer via the binding of identified biomarkers to specific antibodies followed by cross-linking on iron oxide nanoparticles.[120] Finally, detection in microfluidics has been extended to variety of other novel techniques including digital holography based imaging in turbid fluids[121,122] and of organisms,[123] diamagnetic particle based magnetophoresis,[124] near-IR based fluorescence based sensors,[125] bubble-based microfluidic gas sensors,[126] and diffusion-based time capsules.[127]

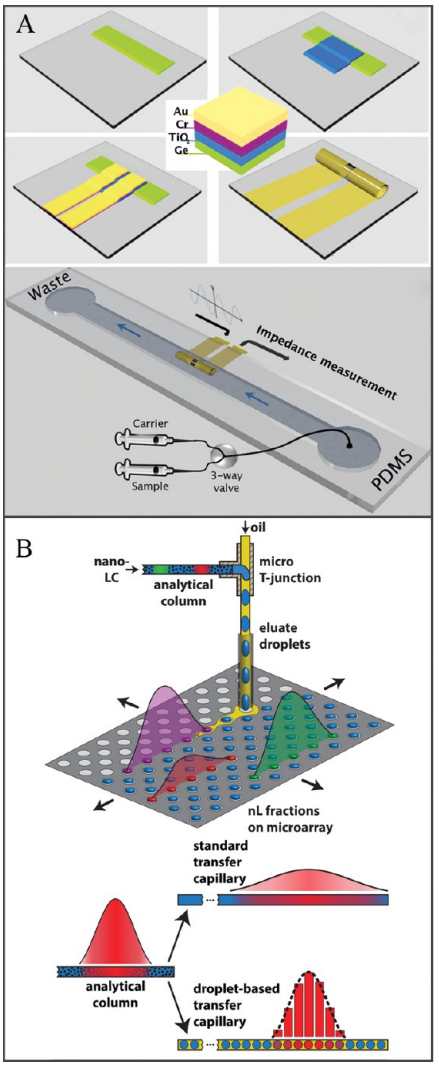

Figure 6. (A) Schematic illustration of fabrication of 3D tubular form Au microsensor and electrode confinement with microfluidic manifold. Thin layers deposition of Ge (20 nm), TiO_2 (60 nm), Cr (5 nm), and Au (10 nm) using conventional photolithography followed by rolling-up technique was used to fabricate tubular structure. Adapted from Martinez-Cisneros, C. S.; Sanchez, S.; Xi, W.; Schmidt, O. G. *Nano Lett.* **2014**, *14*, 2219−2224 (ref 117). Copyright 2014 American Chemical Society. (B) Schematic of integration of droplet-based nanoliquid chromatographic system with microfluidic platform. Reproduced from Kuester, S. K.; Pabst, M.; Jefimovs, K.; Zenobi, R.; Dittrich, P. S. *Anal. Chem.* **2014**, *86*, 4848−4855 (ref 131). Copyright 2014 American Chemical Society.

MICROFLUIDIC PLATFORMS

Integrated Devices. One of the fundamental advantages of microfluidic devices is the ability to integrate multiple chemical processing and fluidic manipulation operations into a small footprint. In many cases an automated sample-in/answer-out system is the ultimate goal. Such systems should provide accurate results in near real time. An example of such a device

DOI: 10.1021/acs.analchem.5b04310
Anal. Chem. 2016, 88, 320−338

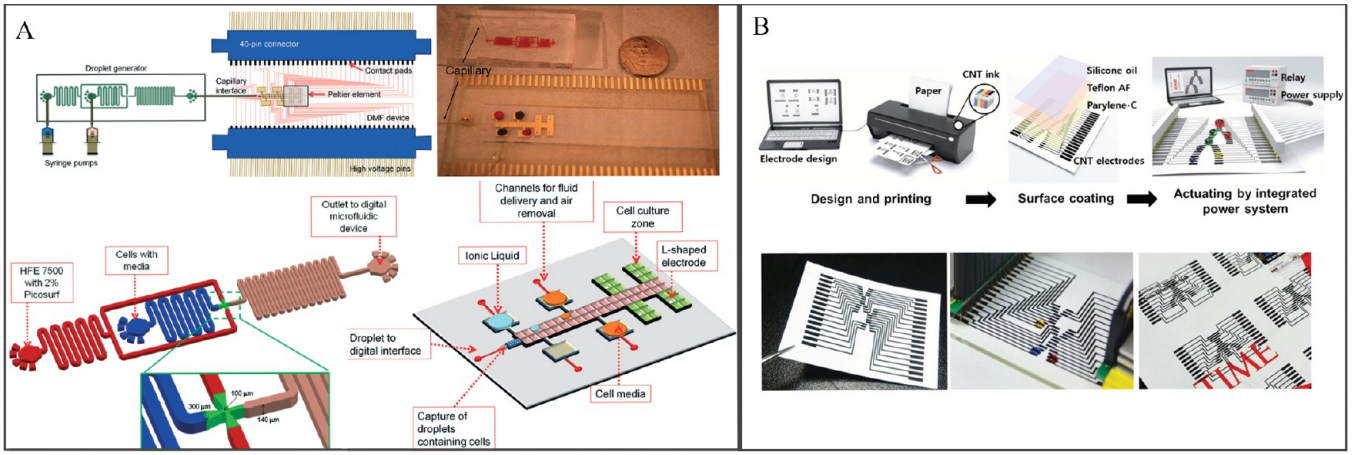

Figure 7. (A) Droplet to Digital (D2D) microfluidic device. Reproduced from Shih, S. C. C.; Gach, P. C.; Sustarich, J.; Simmons, B. A.; Adams, P. D.; Singh, S.; Singh, A. K. *Lab Chip* **2015**, *15*, 225−236 (ref 134), with permission of the Royal Society of Chemistry. (B) Overview of the fabrication process for an active microfluidic paper chip and photograph of a microfluidic paper chip assembled in the integrated switching power system. Reproduced from Active Digital Microfluidic Paper Chips with Inkjet- Printed Patterned Electrodes, Ko, H.; Lee, J.; Kim, Y.; Lee, B.; Jung, C. H.; Choi, J. H.; Kwon, O. S.; Shin, K. *Adv. Mater.*, *26*, 2335−2340 (ref 137). Copyright 2015 Wiley.

to create dried blood samples on commercially available Dried Blood Spot (DBS) cards was reported.[128] Blood obtained from a finger prick was introduced directly into a microfluidic channel and collected on the terminal end as a spot on a DBS card. This approach prevented typical hematocrit problems (i.e., spreading blood on filter papers due to it is viscosity), provided more accurate and reproducible volumes in the range of 5−10 μL compared to conventional micropipetting techniques, and was well suited for use with clinically relevant applications.[128] Another simple approach to sample collection and analysis used an enzyme-immobilized paper microfluidic platform with an enzymeless electrode composed of Pt nanoparticles to detect the activity of glucose oxidase (GOx) via CV.[129]

Integration of automated sample collection, processing, and real time analysis on microfluidic platforms with mass spectrometry continued to show progress.[130] For example, a microextraction system was designed to automatically extract samples from biological matrixes without any pretreatments. This mechanical extraction system was integrated with both MS and a fluorescent microscope in order to monitor the time-resolved extraction progress. This system was demonstrated with samples of tea leaves and selected powdered drugs.[130] As described above in the Surface Modification section, Au NPS were used to concentrate Hg^{2+} in aqueous samples prior to ICPMS analysis.[27] This microfluidic manifold was reusable (>30 samples), eco-friendly, and highly specific toward Hg^{2+} analysis.[27] In another approach, nanoliquid chromatography (nano-LC) eluate was collected using a droplet-based microfluidics device followed by MALDI-MS analysis (Figure 6B).[131] To demonstrate the capabilities of this device, selected peptides were derived from α-casein and bovine serum albumin (BSA) and separated on the nano-LC. Eluate from the nano-LC was encapsulated into oil droplets to limit band dispersion. Thousands of nanoliter fractions from the nano-LC were spotted on a microarray plate. Peak resolution was improved by 50% compared to "direct nanospray-MS coupling" and "continuous-flow spotting onto a standard MALDI target".[131] While there are major advantages to integrating MS detection microfluidics, increasing the system complexity and costs are unavoidable.

Optical detection can also be improved through integration. LIF measurements, for example, can be significantly enhanced by incorporating "arrayed waveguide gratings (AWG)"[132] into the microfluidic manifold. Such a device was recently reported in which simultaneous/successive detection of fluorescent dyes was achieved. In addition, this miniaturized system (1 mm × 1 cm foot print) was portable and provides higher spatial resolution, and results can be obtained in a simple image readout.[132]

Digital Microfluidics. Digital microfluidics (DMF) is an emerging liquid-handling branch of microfluidics that discretely manipulates picoliter- to microliter-sized droplets in integrated microfluidic systems. In DMF, droplets are individually moved and addressed on an open array of electrodes coated by a hydrophobic insulator.[133] DMF systems are particularly attractive for applications requiring low reagent consumption and fast heat transfer. The systems can be easily integrated with other analytical techniques because droplets can be individually made to merge, mix, split, and dispense from reservoirs. To date, reported DMF devices are focused on developing technology for individual cell manipulation, particle sampling and separation, chemical synthesis, and microair bubble manipulation.[134,135] One unique application of DMF was for the analysis of a group of single individual protoplasts and *Arabidopsis thaliana* plants labeled with magnetic particles. This approach enhanced the throughput of water permeability measurements on single protoplasts cells.[136]

DMF integrated with a new hybrid droplet-to-digital microfluidic platform (D2D) was fabricated to perform multistep cellular toxicity assays (Figure 7A). This D2D platform combined two formats, droplets-in-channel and DMF for facile generation of droplets containing single cells and the manipulation of droplets including control of different droplet volumes (pL−μL), respectively. This novel technique allowed the creation of a dilution series of ionic liquids (IL) with parallel single cell culturing and the analysis of IL toxicity screening. Ionic liquid pretreatment technology is a promising method because of its ability to efficiently dissolve and fractionate biomass.[134]

A new fabrication methodology known as an active paper open chip (APOC) allowed a broader range of fluidic

DOI: 10.1021/acs.analchem.5b04310
Anal. Chem. 2016, 88, 320−338

operations to be performed on a paper-based fluidic chip. This approach used printed electrodes and selected coatings to implement electrowetting techniques on paper (Figure 7B).[137] On this APOC, sample drops could be diluted, merged, and mixed with predetermined quantized volumes. The ability to tune the surface tension by using lubricating silicone oil and an ac driving voltage at a low frequency was critical to overcoming the significant limitation posed by low printing resolution.

DMF has recently emerged as a powerful method for sample processing for solid phase extraction (SPE).[138] For example, C18-functionalized magnetic beads were manipulated using an automated DMF direct analysis method for parallel processing.[138] DMF was used in the multiplexed extraction and analysis of pharmaceuticals in dried blood spot (DBS) samples. This is emerging as a valuable technique in the fields of clinical and preclinical testing of pharmaceuticals.[139] Compared to conventional techniques, this method allowed for a 3× reduction in extraction solvent and an order of magnitude reduction in processing time.

Point of Care (POC). POC applications continue to be popular. Several new portable microfluidic devices were reported[140] with multiple integrated functionalities to make simpler,[141] faster,[142] and cheaper[143] devices with better detection limits.[144] Recently, volumetric bar-chart chips (V-chips) have been reported for analyses where a "yes" or "no" answer is desired. These types of devices are portable[140] and provide highly sensitive detection.[144] For example, a V-chip composed of Au@PtNPs encapsulated in a DNA-aptamer-hydrogel matrix was used to examine cocaine in urine.[140] In this device, the interaction of the target (i.e., cocaine) with the aptamer releases the Au@PtNPs which can then decompose H_2O_2 creating O_2 that displaces the ink solution trapped in the middle of the microchannel. This mechanism was used to determine whether the response was "yes" or "no". A similar approach reported the application of competitive N_2 production to distinguish human chorionic gonadotropin (HCG) with ∼1.3-fold concentration difference. In this approach, horseradish peroxidase (HRP) was incorporated into both sample and control. N_2 was then produced using the reaction between luminol, H_2O_2, and HRP. Competitive production of N_2 by the control and the sample at two ends of the microchannel was then used to displace the ink solution and determine whether the test was positive or negative.[144] The device was applied to screening drugs of abuse.

A microfluidic device consisting of 500 channels was designed to rapidly analyze (within 20 min) the DNA integrity of sperm using fluorescent based imaging.[142] Significant increases in bull and human sperm vitality were demonstrated compared to existing techniques.[142] A low cost "intelligent microscale electrochemical device (iMED)"[143] was designed to analyze specific biomarkers associated with the H1N1 virus. In this report, the microfluidic manifold was integrated with a low cost printed electrode platform and a preloaded reagents cartridge was used to introduce reagents in a stepwise manner. Moreover, H1N1 split-influenza-vaccine (H1N1−SV) was detected with the LOD 5 ng/mL via amperometry.[143]

Recently, the coupling of POC devices with smart phones has significantly increased in popularity.[114,145,146] For example, fluid handling in a microfluidic system via pneumatically controllable valves using a smartphone has been reported.[145] The fully automated liquid manipulation was governed by a smartphone app and the system was powered by a 12.8 V and 1500 mA lithium-ion battery.[145] A proof of concept immunoassay for HIV1 P24 was demonstrated.[145] The system dimensions were 6 cm × 10.5 cm × 16.5 cm. Such miniaturization is a good alternative for externally driven pressure sources, syringe pumps, and computer guided fluid manipulations. POC devices have also been developed for a variety of clinically relevant analytes.[147,146,148−151] Several reports focused on enzyme-linked immunosorbent assays (ELISA) in order to perform HIV related detection on miniaturized fluid manipulating systems.[146,147] For example, a microfluidic platform coupled with a smartphone dongle has been utilized to analyze whole blood from 96 volunteer patients. This technique was capable of running multiplex tests in order to evaluate antibody activities for HIV and syphilis and produced results within ∼15 min. The device performance met clinically recommended levels in terms of sensitivity (90−100%) and selectivity (80−100%).[146] Another approach for performing ELISA based HIV clinical trials used a microfluidic platform that was designed to analyze CD4 cells in whole blood.[147] Cells were captured with anti-CD4+ antibodies which were incorporated onto magnetic microbeads. Cells were moved under the influence of a magnetic field and color development was achieved by introducing HRP. In this approach, cell counting and image based analysis was performed with a smartphone.[147] Other POC devices, have focused on nonclinical fields such as food, drinking water, and environmental analysis. For example, square wave voltammetry[152] based and colorimetric[153] based detection of *E. coli* and *S. aureus* bacterial pathogens were carried out using a miniaturized cassette that was composed of polyethylene ribbon containing individually addressable sample reservoirs.[153] The ability to control the temperature of the system provided optimal conditions for the assay. This device was capable of achieving the LODs down to 30 CFU/mL and 200 CFU/mL for *E. coli* and *S. aureus*, respectively.[153]

Centrifugal. Centrifugal microfluidic devices continue to be popular in the clinical analysis arena. A sample-to-answer centrifugal device was developed for the sensitive detection of botulinum toxin.[154] The device used capture beads functionalized with antibodies to immobilize the target antigen, and subsequently a fluorescently labeled detection antibody was bound to the capture bead in the presence of the target. The analyte attached to the capture beads was then purified using density sedimentation and condensed into a pellet for fluorescence detection and quantification. Centrifugal methods have also made their way into genomics. A device capable of forming monodisperse droplets for the encapsulation of recombinase polymerase amplification and quantification of listeria monocytogens was reported.[155] With the use of this centrifugal platform, total analysis time was decreased from 2 h to less than 30 min. In addition to expanded applications, functional elements have also been developed. Multidirectional and actively controlled valving and pumping has proven to be a challenge in centrifugal microfluidics. One group developed an on board active pneumatic control for centrifugal microfluidics.[156] The integration of this active control enabled more complex fluid manipulation such as reverse flow pumping and rapid fluid mixing. (Figure 2G) Additionally, a device capable of selectively releasing four liquids at different times was developed.[157] Each timer functions by overfilling a chamber pneumatically and allowing liquid to slowly flow into a secondary chamber at a previously specified rate. Once all of the liquid has exited the first chamber, the flow rate at the outlet of the second chamber abruptly increases. Another

DOI: 10.1021/acs.analchem.5b04310
Anal. Chem. 2016, 88, 320−338

passive control mechanism was developed by utilizing elastic energy stored within a latex membrane acting as a Micro-balloon.[158] The latex balloon pumps liquid toward the center of the centrifugal device, counter to the centrifugal flow. The volume of liquid pumped can be varied by simply changing the size of the balloon. This offers a relatively facile mechanism for transporting fluid against the centrifugal flow.

World-to-Chip Interface. The ability to interface microfluidic channels with external components or load samples onto microfluidic devices is often an issue. Recently simplifying and improving this interface has been addressed with 3D printing methods that incorporate interconnects when printing the microfluidic device as described above.[19,20] To improve sample collection and in particular blood collection, a simple self-powered disposable polymer microneedle was fabricated in order to collect the blood with finger prick.[159] In this technique, a prevacuumed PDMS actuator was used to provide the required power without using any external sources.

APPLICATIONS

The overall usefulness and applicability of microfluidics to real life chemical analysis issues is reflected in the large number and variety of reports published in this area. While applications focusing on single cell analysis dominate the literature many other applications in the areas of drug screening, drug discovery, genetics, proteomics, environmental health and safety, and food and water quality abound. One area of particular interest that has received increased attention over the last 2 years is the analysis of microbiomes. Microfluidics is now making contributions in this area also.

Drug Screening and Drug Discovery. The small volumes, high throughput, biocompatibility, and multiplexing capability of microfluidic systems provide many advantages for drug screening and drug discovery applications.[160] A significant amount of money is lost in the drug development pipeline because toxicity and efficacy are not detected early enough in the process. This is especially true for drug-induced hepatotoxicity. To address this issue, a recent digital microfluidic platform was reported for liver disease related drug discovery.[161] This microfluidic organoid device for drug screening (MODS) platform used cocultures of HepG2 and NIH-3T3 cells to demonstrate the hepatotoxicity of acetaminophen. The authors claim that the platform was a better mimic of *in vivo* liver tissue than a 2D cell culture. Other approaches to drug discovery have focused on high-throughput screening. For example, a high throughput,[162] fully automated drug screening microfluidic device was used to encapsulate genetically modified bacteria and pathogens together in ~25 pL agarose hydrogel drops. The agarose drops were emulsed in oil and the bacteria were modified to secrete potentially lytic compounds. The droplets were then sorted using FACS based upon whether the pathogen was lysed. This device generated throughputs of 3 000 droplets/s.[162] In addition to drug discovery, it is important to evaluate toxicity of drugs for better treatments. A clinically applicable, miniaturized version of such system has been designed to examine cytotoxicity of anticancer drugs.[163] In this device, fluid manipulation was performed via peristaltic pumps and detection was performed using impedance spectroscopy for real time analysis.[163] Another system consisted of 3D trapping sites with an integrated ITO heating element to maintain optimum temperatures (Figure 8A). Piezoelectric pumps were used to generate fluid pumping, and trapping was performed using low-pressure suction. In order to achieve full automation, device adjustments were made using a computer guided robotic arm. A proof of concept experiment was performed by trapping and culturing zebrafish embryos.[164] Finally a microfluidics-based multisensor cell culturing system for both drug screening and cancer cell monitoring was reported.[165] This system included integrated pH, oxygen, glucose and lactate sensors. Microphysiometry data was obtained using this system on T98G brain cancer cells. Changes in cell metabolism could be monitored during drug screens.

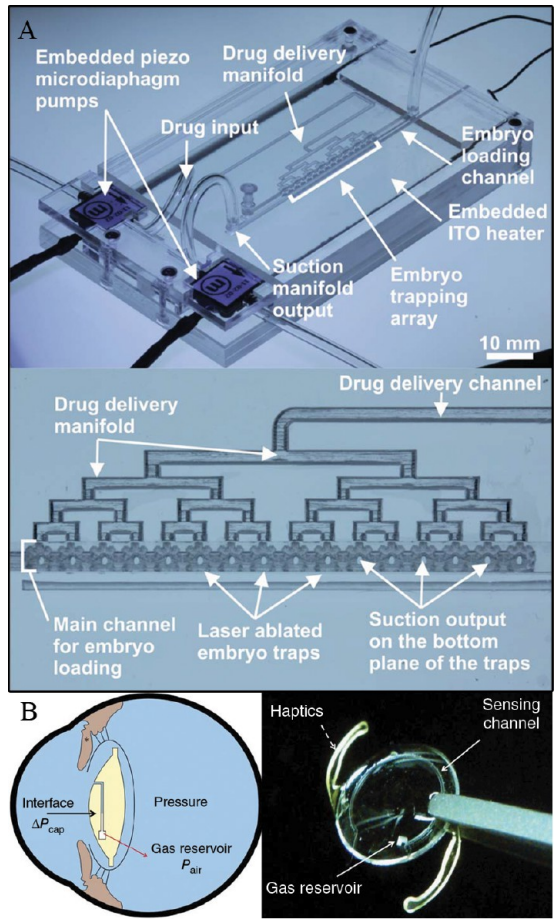

Figure 8. (A) Overview of multilayer microfluidic device for trapping and culturing zebrafish embryos and a magnified view of multiple cell trapping sites and drug delivery microfluidic structure. Reproduced from Integrated chip-based physiometer for automated fish embryo toxicity biotests in pharmaceutical screening and ecotoxicology, Akagi, J.; Zhu, F.; Hall, C. J.; Crosier, K. E.; Crosier, P. S.; Wlodkowic, D. *Cytometry Part A, 85A*, 537−547 (ref 164). Copyright 2015 Wiley. (B) Implantable microfluidic device to monitor intraocular pressure of the eyes of glaucoma patients. Reproduced from Araci, I. E.; Su, B.; Quake, S. R.; Mandel, Y. *Nat. Med. 20*, 1074−1078 (ref 194). Copyright 2015 The Nature Publishing Group.

Disease Diagnosis. The ability to detect rare cells in a population is critically important to diagnosing diseases early. Many microfluidic devices have been reported that use a variety of methods to pull rare cells out of a sample some of which have already been discussed above and those focused on detection using genetic markers are discussed in the Nucleic Acid Analysis section below. In a novel approach to isolating rare pathogen cells in blood, a microfluidic device was reported that used magnetic beads to isolate fungal pathogens. In order to overcome the typical problem of the excess magnetic beads

DOI: 10.1021/acs.analchem.5b04310
Anal. Chem. 2016, 88, 320−338

obscuring optical detection, the chip contained an array of depressions spread out along the channel under the capture magnet. This array successfully spread out the beads more effectively and allowed a greater number of pathogens to be detected. With this technique the LOD was <1 pathogen cell/mL of blood.[58]

Nucleic Acid Analysis. The detection of nucleic acids via microarrays with or without PCR has been a popular application for microfluidic systems for many years. A wide variety of genetic amplification techniques have been developed and reported beyond PCR and qPCR (quantitative PCR) on microfluidic devices, including recombinase polymerase amplification (RPA), rolling circle amplification (RCA), and nucleic acid sequence-based amplification (NASBA).

In the previous 2 years, fundamental improvements in DNA purification and amplification have been reported along with the application of integrated microfluidic devices to the genetic analysis of various organisms and environments.

While the first report of PCR performed on a microfluidic device was published more than 15 years ago, there are still some challenges to performing rapid thermal cycling in small volume microfluidic chambers. One challenge in particular is that the chamber should be closed to the outside world in order to prevent contamination and evaporative losses. Closed systems, however, can interfere with the mechanical stability of the device. In order to overcome such issues, a recently reported paper used a vapor-diffusion barrier integrated in a centrifugal microfluidics device in order to lower the pressure from 100 kPa down to only 35 kPa.[166] The chamber was easily integrated with other DNA processing steps on the chip. Another issue of crucial importance is how to isolate and purify DNA from potential interfering species. One method to address these challenges used a Fusion 5 filter and PDMS membrane sandwiched between two PMMA layers.[167] This DNA extractor was combined with an upstream 80 μm membrane to extract and purify DNA from a several different samples including whole blood. PCR could then be performed directly on the filter disk either in situ or by removing it and placing it in a conventional PCR device. Complete extraction required only 8 min. In another report, a shear modulated inertial microfluidics sample processing approach was used to enrich malaria parasites from whole blood for qPCR analysis.[168] This device consisted of a channel with regular contractions and expansions to focus the parasites into a narrow stream to separate them from white blood cells. The device was shown to have 100× better LODs than the current gold standard for malaria detection. PCR was also combined with deep sequencing (mmPCR-seq) on a microfluidic device to provide a rapid and economical method of measuring allelic ratios in low-quality and low-quantity RNA samples.[169]

A variety of amplification and array techniques integrated into microfluidic devices have been reported for the detection of diseases and pathogens as described below. Digital PCR (dPCR) has become popular because of its increased precision compared to traditional PCR and is routinely used for clonal amplification in next generation sequencing applications. In order to perform dPCR one needs to be able to create and load an array of amplification chambers. To simplify the design and loading of such chambers, a valve-free and power free design was developed.[170] This chip had >5000, 5 nL chambers that were automatically filled by taking advantage of PDMS's gas permeability and creating partial vacuums in the chambers by lowering the pressure surrounding the chip. Both reagents and a sealing oil were pulled in using this method. The device was successfully demonstrated using a lung cancer gene. The system also simplified the real world-to-chip connections for sample loading. The ability to perform qPCR on single cells in droplets enables such droplets to be sorted based upon the qPCR results. A recent paper reported the dielectrophoretic sorting of such single cell containing drops on a microfluidic device after off-chip qPCR amplification.[171] The technique was called PCR-activated cell sorting (PACS). Over 100 000 prostate cancer cells were sorted using PACS based upon the presence of vimentin mRNA. Compared to fluorescence *in situ* hybridization-flow cytometry (FISH-FC), PACS does not require cell fixation so cellular constituents in the isolated droplets could be interrogated for further study. Another amplification technique, rolling circle amplification (RCA) was applied to the detection of thrombin.[172] The thrombin was isolated using an aptamer and a second thrombin aptamer with a G-quadruplex template was used to amplify the single using RCA. The detection limit was 0.083 pg/mL from thrombin in plasma and serum.

The ability to use simple, inexpensive, and portable microfluidic systems for the detection of pathogens in water and other samples has significant real world impact in resource poor areas. For example the integration of a nucleic acid sequence-based amplification (NASBA) method into a microfluidic device allowed the detection of only 30 *C. parvum* oocysts.[173] In this PMMA device, the surface was UV/ozone treated to attach a fifth generation PAMAM dendrimer. After the NASBA, primers were attached to the PAMAM, the channels were rinsed with sample followed by the NASBA buffer. The detection limits were significantly better than previously reported NASBA implementations on microfluidic devices. A multiplexed on-chip recombinase polymerase amplification system was reported that amplified specific target sequences from several important pathogenic bacteria.[174] Results from this device could be generated in <20 min, and the detection limits were 10 CFUs for MRSA and 100 CFUs for *Salmonella* and *Neisseria* bacteria. Another microfluidic device was used to clear bacteria from blood using magnetic nanoparticles modified with bis-Zn-DPA that are bound to both Gram-positive and Gram-negative strains.[175] Magnets were used to pull the particles and attached bacteria from the blood. The technique could operate at flow rates of up to 60 mL/h with close to 100% clearance.

Hybridization Microarrays. Another area of interest especially in Europe is the detection of genetically modified organisms. A recently reported microfluidic system integrated microchip-PCR with a microarray system to detect GMOs.[176] The system contained multiple amplicons allowing for the analysis of 91 targets that covered ∼97% of all commercialized genetically modified products. The results were 100% accurate with LODs suitable for real world applications. In another report, a method was developed for the rapid detection of nervous necrosis virus (NNV) and iridovirus in fish using a multiwell microfluidic device.[177] The device was loaded with virus containing samples mixed with probes conjugated to magnetic beads and molecular beacons. A thermal denaturing and annealing cycle followed by capture using a magnet allowed the detection of the virus in samples in <30 min with detection limits suitable for practical applications.

In an interesting twist on bar-coding, a microfluidic device was reported that used an array of parallel channels of various widths with various spacings.[178] Protein or nucleic acid assays carried out in the channel manifold created colored precipitates

DOI: 10.1021/acs.analchem.5b04310
Anal. Chem. 2016, 88, 320−338

that replicated a barcode that was read out using a smartphone app. The practicality of this approach was demonstrated using HIV and other pathogen samples.

Microbiomes and Environmental Changes. Microfluidic devices were used to create miniature environments for either culturing organisms[179] or for monitoring environmental changes. Microbiome studies, and human microbiome studies in particular, have generated substantial interest over the past few years with the realization of how important these microbial communities are to human health. Most organisms in these communities, however, cannot be grown under standard culturing conditions. A novel approach to determining appropriate culturing conditions was recently reported using a combination of standard and microfluidic methods.[180] A microfluidic SlipChip with 3200, 6 nL wells was used to cultivate microorganisms from a gut microbiome community. The small volume of the SlipChip allowed it to be used in an anaerobic chamber and was compatible with sample splitting and PCR. The use of this microfluidic system allowed the first targeted cultivation of a high-priority microorganism group as part of the Human Microbiome project. A second report used a microfluidic system to study proximal and distal bacterial communication in a simulated intestinal tract.[179] In another application, a microfluidic device was used to examine the spatial ecology and competition between populations of marine bacterioplankton.[181] The microfluidic systems were used to generate a temporally varying nutrient landscape and to monitor the chemotactic movement of the populations. The varying responses of the organisms may help better understand gene flow and differentiation.

Moving out of the realm of living organisms, microfluidic devices can also be used to understand chemical and physical transformations that have important environmental and industrial consequences. For example, the dewpoints of supercritical CO_2 were directly observed in a microfluidic device under pressures, concentrations, and temperatures that were industrially relevant.[182] This technique required only ~10 μL and could be used under ultralow water conditions that have limited previously reported methods. Several devices were reported which focused on detecting a pollutants in water including NO_3^-,[183] PAHs,[184] pH,[185] NH_3,[185] Pb^{2+},[186] and *E. coli*.[187−190]

Chemotaxis. Chemotaxis is the ability of an organism to move along a chemical gradient. Microfluidic devices are especially good at creating stable chemical concentration gradients because of their laminar flow properties as discussed above. As such, several unique microfluidic devices have been reported that generate gradients of chemoattractants to study the movement of organisms in response to them. For example, a microfluidic device was recently reported that could be used to discriminate between asthma and allergic rhinitis based upon neutrophil chemotaxis. The neutrophils were isolated from whole blood and the gradient was generated using a reagent in lid configuration.[191] The device was hand-held and could perform a diagnosis in ~5 min. In another microfluidic chemotaxis assay, a biohybrid drug delivery device was tested.[192] This drug delivery device consisted of a polymeric microparticle with motile bacteria attached. The ability of the bacteria to propel the particle up a stable chemoattractant gradient in a microfluidic channel was monitored. These experiments showed that the chemoattractant gradient was much more important than particle shape. Organisms are not the only entities that can follow a chemical concentration gradient. In an intriguing paper, the ability to separate active from nonactive enzymes along a stable gradient of substrate in a simple microfluidic device was demonstrated.[193] In this experiment, active enzymes preferentially migrated up the stable concentration gradient allowing them to be separated from nonactive enzymes.

Extreme Environments. Each year there are always a few microfluidic devices that are developed to work in unusual environments. For example, a microfluidic device was reported for use in the eye to monitor intraocular pressure (Figure 8B).[194] This device was an intraocular lens with a small gas reservoir and a 50 μm channel that could measure pressure changes in the eye down to 1 mmHg. This device could be implanted during cataract surgery and used to monitor glaucoma. Detection was performed using a smartphone app. In a slightly farther out application, a nonaqueous capillary electrophoresis separation with an LIF detection system was developed to separate and identify primary amines in Titan (moon of Jupiter) aerosol analogues.[195] This device could operate at temperatures down to −20 °C. It has provided the first step in better understanding the atmosphere of Titan.

Protein Analysis. The ability to detect disease biomarkers at low concentrations both cheaply and rapidly without the need of specially trained personnel and expensive equipment would allow earlier detection and better patient prognosis. ELISAs are currently the gold standard when it comes to detecting low levels of proteins. ELISAs however have several limitations including specificity issues and the need for moderately complex instrumentation to perform the analysis. Simpler microfluidic systems could make the detection of low protein levels easier and cheaper. Recently a digital microfluidic platform that seeks to accomplish these goals has been reported.[196] The device consisted of a capture section to pull down the protein, followed by interaction with antibody-coated particles. The particles were then released the detected using an integrated impedance sensor. This device was able to both quantify protein levels and activities with a LOD of 50 pM which is about 10× better than that a comparable ELISA assay.

■ CONCLUSIONS AND OUTLOOKS

The total number of papers in the area of microfluidics continues to increase steadily. This has resulted in the need for multiple reviews focusing on specific areas in the broader context of microfluidics, hence, the addition of reviews in this journal on paper microfluidics, droplet-based microfluidics, and cellular analysis on microfluidic devices. The past 2 years have especially seen an increase in the number of papers focusing on paper microfluidics with special attention to the integration of separations on these devices with detection. A couple of other significant trends is the increasing popularity of 3D printing in the fabrication of microfluidic devices, the application of new particle and fluidic manipulation mechanisms (e.g., acoustophoresis), and the integration of microfluidics with smart phones and smart phone apps for both detection (read-out) and device control. Outside of droplet and single cell analysis applications that were reviewed elsewhere, there was a significant increase in the use of microfluidic devices for drug screening and disease diagnosis and the first applications of microfluidics to the analysis of microbiomes.

DOI: 10.1021/acs.analchem.5b04310
Anal. Chem. 2016, 88, 320−338

AUTHOR INFORMATION

Corresponding Author

*E-mail: culbert@ksu.edu. Phone: +1-785-532-6685. Fax: +1-785-532-6666.

Author Contributions

All authors contributed to the writing of the manuscript and have approved the final version.

Notes

The authors declare no competing financial interest.

Biographies

Damith E. W. Patabadige received his B.S. degree in Chemistry from University of Colombo, Sri Lanka in 2006. He is currently a Ph.D. candidate in Department of Chemistry at Kansas State University. His current research is focused on integration of fiber optics with multilayer microfluidic devices for single cell analysis and studying reactive nitrogen/oxygen species in Jurkat cells.

Shu Jia received his B.S. degree in Sun Yat-sen University in 2014. He is currently a graduate student in Chemistry Department at Kansas State University. His current research focuses on droplet microfluidic manipulation and calibration.

Jay Sibbitts received his B.S. degree in Chemistry from Truman State University in 2014. He is currently a graduate student in the Chemistry Department at Kansas State University. He is currently researching the applications of dielectric elastomeric actuators.

Jalal Sadeghi received his M.S. degree in Laser Physics from Shahid Beheshti University, Tehran, Iran, in 2012. He is currently a Ph.D. candidate at Laser and Plasma Research Institute at Shahid Beheshti University. He is collaborating with the Department of Chemistry at Kansas State University on cytometric analysis of cells and particles based on integrated optics.

Kathleen Sellens received her B.S. in Chemistry from McKendree University in 2012. Currently, she is a Ph.D. candidate in the Chemistry Department at the Kansas State University. Her research focuses on isolating *Anopheles gambiae* immune response protein complexes using capillary immunoaffinity chromatography.

Christopher T. Culbertson received a Ph.D. in Chemistry from the University of North Carolina at Chapel Hill in 1991 followed by a postdoctoral fellowship at Oak Ridge National Laboratory. He is presently an Associate Professor in the Chemistry Department at Kansas State University.

ACKNOWLEDGMENTS

This research was funded by NSF Grant CHE-1411993. D.E.W.P. was supported by the Terry Johnson Cancer Center, Kansas State University.

REFERENCES

(1) Reyes, D. R.; Iossifidis, D.; Auroux, P.-A.; Manz, A. *Anal. Chem.* **2002**, *74*, 2623.
(2) Culbertson, C. T.; Mickleburgh, T. G.; Stewart-James, S. A.; Sellens, K. A.; Pressnall, M. *Anal. Chem.* **2014**, *86*, 95.
(3) Jackson, J. M.; Witek, M. A.; Hupert, M. L.; Brady, C.; Pullagurla, S.; Kamande, J.; Aufforth, R. D.; Tignanelli, C. J.; Torphy, R. J.; Yeh, J. J.; Soper, S. A. *Lab Chip* **2014**, *14*, 106.
(4) Mazurek, P.; Daugaard, A. E.; Skolimowski, M.; Hvilsted, S.; Skov, A. L. *RSC Adv.* **2015**, *5*, 15379.
(5) Zhang, W.; Tullier, M. P.; Patel, K.; Carranza, A.; Pojman, J. A.; Radadia, A. D. *Lab Chip* **2015**, *15*, 4227.
(6) Bomer, J. G.; Prokofyev, A. V.; van den Berg, A.; Le Gac, S. *Lab Chip* **2014**, *14*, 4461.
(7) Rose, S.; Prevoteau, A.; Elziere, P.; Hourdet, D.; Marcellan, A.; Leibler, L. *Nature* **2014**, *505*, 382.
(8) Uba, F. I.; Hu, B.; Weerakoon-Ratnayake, K.; Oliver-Calixte, N.; Soper, S. A. *Lab Chip* **2015**, *15*, 1038.
(9) Cassano, C. L.; Simon, A. J.; Liu, W.; Fredrickson, C.; Fan, Z. H. *Lab Chip* **2015**, *15*, 62.
(10) Lee, K. G.; Shin, S.; Il Kim, B.; Bae, N. H.; Lee, M.-K.; Lee, S. J.; Lee, T. J. *Lab Chip* **2015**, *15*, 1412.
(11) Konda, A.; Taylor, J. M.; Stoller, M. A.; Morin, S. A. *Lab Chip* **2015**, *15*, 2009.
(12) Wasay, A.; Sameoto, D. *Lab Chip* **2015**, *15*, 2749.
(13) Comina, G.; Suska, A.; Filippini, D. *Lab Chip* **2014**, *14*, 2978.
(14) Au, A. K.; Lee, W.; Folch, A. *Lab Chip* **2014**, *14*, 1294.
(15) Lee, W.; Kwon, D.; Chung, B.; Jung, G. Y.; Au, A.; Folch, A.; Jeon, S. *Anal. Chem.* **2014**, *86*, 6683.
(16) Shallan, A. I.; Smejkal, P.; Corban, M.; Guijt, R. M.; Breadmore, M. C. *Anal. Chem.* **2014**, *86*, 3124.
(17) Huang, T. Q.; Qu, X.; Liu, J.; Chen, S. *Biomed. Microdevices* **2014**, *16*, 127.
(18) Gelber, M. K.; Bhargava, R. *Lab Chip* **2015**, *15*, 1736.
(19) Paydar, O. H.; Paredes, C. N.; Hwang, Y.; Paz, J.; Shah, N. B.; Candler, R. N. *Sens. Actuators, A* **2014**, *205*, 199.
(20) Erkal, J. L.; Selimovic, A.; Gross, B. C.; Lockwood, S. Y.; Walton, E. L.; McNamara, S.; Martin, R. S.; Spence, D. M. *Lab Chip* **2014**, *14*, 2023.
(21) Dirany, M.; Dies, L.; Restagno, F.; Leger, L.; Poulard, C.; Miquelard-Garnier, G. *Colloids Surf., A* **2015**, *468*, 174.
(22) Kovach, K. M.; Capadona, J. R.; Sen Gupta, A.; Potkay, J. A. *J. Biomed. Mater. Res., Part A* **2014**, *102*, 4195.
(23) Huang, C. J.; Chang, Y. C. *Materials* **2014**, *7*, 130.
(24) Jang, M.; Park, C. K.; Lee, N. Y. *Sens. Actuators, B* **2014**, *193*, 599.
(25) Kitsara, M.; Nwankire, C. E.; Walsh, L.; Hughes, G.; Somers, M.; Kurzbuch, D.; Zhang, X.; Donohoe, G. G.; O'Kennedy, R.; Ducree, J. *Microfluid. Nanofluid.* **2014**, *16*, 691.
(26) Zilio, C.; Sola, L.; Damin, F.; Faggioni, L.; Chiari, M. *Biomed. Microdevices* **2014**, *16*, 107.
(27) Hsu, K.-C.; Lee, C.-F.; Tseng, W.-C.; Chao, Y.-Y.; Huang, Y.-L. *Talanta* **2014**, *128*, 408.
(28) Oliver-Calixte, N. J.; Uba, F. I.; Battle, K. N.; Weerakoon-Ratnayake, K. M.; Soper, S. A. *Anal. Chem.* **2014**, *86*, 4447.
(29) Batz, N. G.; Mellors, J. S.; Alarie, J. P.; Ramsey, J. M. *Anal. Chem.* **2014**, *86*, 3493.
(30) Liang, R.-P.; Wang, X.-N.; Liu, C.-M.; Meng, X.-Y.; Qiu, J.-D. *J. Chromatogr A* **2014**, *1323*, 135.
(31) Zhou, J.; Pang, H. F.; Garcia-Gancedo, L.; Iborra, E.; Clement, M.; De Miguel-Ramos, M.; Jin, H.; Luo, J. K.; Smith, S.; Dong, S. R.; Wang, D. M.; Fu, Y. Q. *Microfluid. Nanofluid.* **2015**, *18*, 537.
(32) Rezk, A. R.; Friend, J. R.; Yeo, L. Y. *Lab Chip* **2014**, *14*, 1802.
(33) Huang, P.-H.; Nama, N.; Mao, Z.; Li, P.; Rufo, J.; Chen, Y.; Xie, Y.; Wei, C.-H.; Wang, L.; Huang, T. J. *Lab Chip* **2014**, *14*, 4319.
(34) Dentry, M. B.; Friend, J. R.; Yeo, L. Y. *Lab Chip* **2014**, *14*, 750.
(35) Collignon, S.; Friend, J.; Yeo, L. *Lab Chip* **2015**, *15*, 1942.
(36) Shilton, R. J.; Travagliati, M.; Beltram, F.; Cecchini, M. *Adv. Mater.* **2014**, *26*, 4941.
(37) Chen, Y.; Nawaz, A. A.; Zhao, Y.; Huang, P.-H.; McCoy, J. P.; Levine, S. J.; Wang, L.; Huang, T. J. *Lab Chip* **2014**, *14*, 916.
(38) Destgeer, G.; Ha, B. H.; Jung, J. H.; Sung, H. J. *Lab Chip* **2014**, *14*, 4665.
(39) Destgeer, G.; Ha, B. H.; Park, J.; Jung, J. H.; Alazzam, A.; Sung, H. J. *Anal. Chem.* **2015**, *87*, 4627.
(40) Bussonniere, A.; Miron, Y.; Baudoin, M.; Matar, O. B.; Grandbois, M.; Charette, P.; Renaudin, A. *Lab Chip* **2014**, *14*, 3556.
(41) Li, P.; Mao, Z.; Peng, Z.; Zhou, L.; Chen, Y.; Huang, P.-H.; Truica, C. I.; Drabick, J. J.; El-Deiry, W. S.; Dao, M.; Suresh, S.; Huang, T. J. *Proc. Natl. Acad. Sci. U. S. A.* **2015**, *112*, 4970.
(42) Ding, X.; Peng, Z.; Lin, S.-C. S.; Geri, M.; Li, S.; Li, P.; Chen, Y.; Dao, M.; Suresh, S.; Huang, T. J. *Proc. Natl. Acad. Sci. U. S. A.* **2014**, *111*, 12992.

DOI: 10.1021/acs.analchem.5b04310
Anal. Chem. 2016, 88, 320−338

(43) Begolo, S.; Zhukov, D. V.; Selck, D. A.; Li, L.; Ismagilov, R. F. *Lab Chip* **2014**, *14*, 4616.
(44) Gao, M.; Gui, L. *Lab Chip* **2014**, *14*, 1866.
(45) Sciambi, A.; Abate, A. R. *Lab Chip* **2014**, *14*, 2605.
(46) Tang, S.-Y.; Khoshmanesh, K.; Sivan, V.; Petersen, P.; O'Mullane, A. P.; Abbott, D.; Mitchell, A.; Kalantar-zadeh, K. *Proc. Natl. Acad. Sci. U. S. A.* **2014**, *111*, 3304.
(47) Cooksey, G. A.; Atencia, J. *Lab Chip* **2014**, *14*, 1665.
(48) Zhang, X.; Xiang, N.; Tang, W.; Huang, D.; Wang, X.; Yi, H.; Ni, Z. *Lab Chip* **2015**, *15*, 3473.
(49) Kim, H.; Kim, J. *Microfluid. Nanofluid.* **2014**, *16*, 623.
(50) Kwa, T.; Zhou, Q.; Gao, Y.; Rahimian, A.; Kwon, L.; Liu, Y.; Revzin, A. *Lab Chip* **2014**, *14*, 1695.
(51) Huang, S.-B.; Zhao, Y.; Chen, D.; Lee, H.-C.; Luo, Y.; Chiu, T.-K.; Wang, J.; Chen, J.; Wu, M.-H. *Sens. Actuators, B* **2014**, *190*, 928.
(52) Kazemzadeh, A.; Ganesan, P.; Ibrahim, F.; Aeinehvand, M. M.; Kulinsky, L.; Madou, M. J. *Sens. Actuators, B* **2014**, *204*, 149.
(53) Hou, X.; Hu, Y.; Grinthal, A.; Khan, M.; Aizenberg, J. *Nature* **2015**, *519*, 70.
(54) Xu, S.; Zhang, Y.; Jia, L.; Mathewson, K. E.; Jang, K.-I.; Kim, J.; Fu, H.; Huang, X.; Chava, P.; Wang, R.; Bhole, S.; Wang, L.; Na, Y. J.; Guan, Y.; Flavin, M.; Han, Z.; Huang, Y.; Rogers, J. A. *Science* **2014**, *344*, 70.
(55) Song, J. L.; Au, K. H.; Huynh, K. T.; Packman, A. I. *Biotechnol. Bioeng.* **2014**, *111*, 597.
(56) Choi, E.; Kwon, K.; Lee, S. J.; Kim, D.; Park, J. *Lab Chip* **2015**, *15*, 1794.
(57) Li, Y.; Liu, C.; Feng, X.; Xu, Y.; Liu, B.-F. *Anal. Chem.* **2014**, *86*, 4333.
(58) Cooper, R. M.; Leslie, D. C.; Domansky, K.; Jain, A.; Yung, C.; Cho, M.; Workman, S.; Super, M.; Ingber, D. E. *Lab Chip* **2014**, *14*, 182.
(59) Pivetal, J.; Toru, S.; Frenea-Robin, M.; Haddour, N.; Cecillon, S.; Dempsey, N. M.; Dumas-Bouchiat, F.; Simonet, P. *Sens. Actuators, B* **2014**, *195*, 581.
(60) Otieno, B. A.; Krause, C. E.; Latus, A.; Chikkaveeraiah, B. V.; Faria, R. C.; Rusling, J. F. *Biosens. Bioelectron.* **2014**, *53*, 268.
(61) Glynn, M.; Kirby, D.; Chung, D.; Kinahan, D. J.; Kijanka, G.; Ducree, J. *JALA* **2014**, *19*, 285.
(62) Shen, S.; Ma, C.; Zhao, L.; Wang, Y.; Wang, J.-C.; Xu, J.; Li, T.; Pang, L.; Wang, J. *Lab Chip* **2014**, *14*, 2525.
(63) Wang, G.; Shi, G.; Wang, H.; Zhang, Q.; Li, Y. *Adv. Funct. Mater.* **2014**, *24*, 1017.
(64) Wang, C.; Ouyang, J.; Wang, Y.-Y.; Ye, D.-K.; Xia, X.-H. *Anal. Chem.* **2014**, *86*, 3216.
(65) Leichle, T.; Bourrier, D. *Lab Chip* **2015**, *15*, 833.
(66) Zhang, J.; Yan, S.; Sluyter, R.; Li, W.; Alici, G.; Nguyen, N.-T. *Sci. Rep.* **2014**, *4*, 4527.
(67) Zhu, T.; Cheng, R.; Liu, Y.; He, J.; Mao, L. *Microfluid. Nanofluid.* **2014**, *17*, 973.
(68) Sciambi, A.; Abate, A. R. *Lab Chip* **2015**, *15*, 47.
(69) Saylor, R. A.; Reid, E. A.; Lunte, S. M. *Electrophoresis* **2015**, *36*, 1912.
(70) Trouillon, R.; Gijs, M. A. M. *Lab Chip* **2014**, *14*, 2929.
(71) Dossi, N.; Toniolo, R.; Impellizzieri, F.; Bontempelli, G. *J. Electroanal. Chem.* **2014**, *722*, 90.
(72) Dossi, N.; Toniolo, R.; Piccin, E.; Susmel, S.; Pizzariello, A.; Bontempelli, G. *Electroanalysis* **2013**, *25*, 2515.
(73) Dimaki, M.; Vergani, M.; Heiskanen, A.; Kwasny, D.; Sasso, L.; Carminati, M.; Gerrard, J. A.; Emneus, J.; Svendsen, W. E. *Sensors* **2014**, *14*, 9505.
(74) Medina-Sanchez, M.; Miserere, S.; Morales-Narvaez, E.; Merkoci, A. *Biosens. Bioelectron.* **2014**, *54*, 279.
(75) Li, L.; Xu, J.; Zheng, X.; Ma, C.; Song, X.; Ge, S.; Yu, J.; Yan, M. *Biosens. Bioelectron.* **2014**, *61*, 76.
(76) Gu, S.; Lu, Y.; Ding, Y.; Li, L.; Song, H.; Wang, J.; Wu, Q. *Biosens. Bioelectron.* **2014**, *55*, 106.
(77) Wu, S.; Zhou, Z.; Xu, L.; Su, B.; Fang, Q. *Biosens. Bioelectron.* **2014**, *53*, 148.
(78) Wu, M.-S.; Liu, Z.; Shi, H.-W.; Chen, H.-Y.; Xu, J.-J. *Anal. Chem.* **2015**, *87*, 530.
(79) Lee, S.; Kang, S. H. *J. Biomed. Nanotechnol.* **2014**, *10*, 2620.
(80) Pires, N. M. M.; Dong, T.; Hanke, U.; Hoivik, N. *Sensors* **2014**, *14*, 15458.
(81) Hung, T. Q.; Sun, Y.; Poulsen, C. E.; Linh-Quyen, T.; Chin, W. H.; Bang, D. D.; Wolff, A. *Lab Chip* **2015**, *15*, 2445.
(82) Hou, J.; Zhang, H.; Yang, Q.; Li, M.; Song, Y.; Jiang, L. *Angew. Chem., Int. Ed.* **2014**, *53*, 5791.
(83) Kim, M.; Pan, M.; Gai, Y.; Pang, S.; Han, C.; Yang, C.; Tang, S. K. Y. *Lab Chip* **2015**, *15*, 1417.
(84) Zhang, Y. S.; Ribas, J.; Nadhman, A.; Aleman, J.; Selimovic, S.; Lesher-Perez, S. C.; Wang, T.; Manoharan, V.; Shin, S.-R.; Damilano, A.; Annabi, N.; Dokmeci, M. R.; Takayama, S.; Khademhosseini, A. *Lab Chip* **2015**, *15*, 3661.
(85) Ozcelik, D.; Parks, J. W.; Wall, T. A.; Stott, M. A.; Cai, H.; Parks, J. W.; Hawkins, A. R.; Schmidt, H. *Proc. Natl. Acad. Sci. U. S. A.* **2015**, *112*, 12933.
(86) Choi, J.; Kang, M.; Jung, J. H. *Sci. Rep.* **2015**, *5*, 15983.
(87) Liu, S.; Wall, T. A.; Ozcelik, D.; Parks, J. W.; Hawkins, A. R.; Schmidt, H. *Chem. Commun. (Cambridge, U. K.)* **2015**, *51*, 2084.
(88) Cheung, M. C.; McKenna, B.; Wang, S. S.; Wolf, D.; Ehrlich, D. J. *Cytometry, Part A* **2015**, *87*, 541.
(89) Han, Y.; Lo, Y.-H. *Sci. Rep.* **2015**, *5*, 13267.
(90) Holzmeister, P.; Pibiri, E.; Schmied, J. J.; Sen, T.; Acuna, G. P.; Tinnefeld, P. *Nat. Commun.* **2014**, *5*, 5356.
(91) Punj, D.; Regmi, R.; Devilez, A.; Plauchu, R.; Moparthi, S. B.; Stout, B.; Bonod, N.; Rigneault, H.; Wenger, J. *ACS Photonics* **2015**, *2*, 1099.
(92) Regmi, R.; Al Balushi, A. A.; Rigneault, H.; Gordon, R.; Wenger, J. *Sci. Rep.* **2015**, *5*, 15852.
(93) Flauraud, V.; van Zanten, T. S.; Mivelle, M.; Manzo, C.; Garcia Parajo, M. F.; Brugger, J. *Nano Lett.* **2015**, *15*, 4176.
(94) Akselrod, G. M.; Argyropoulos, C.; Hoang, T. B.; Ciraci, C.; Fang, C.; Huang, J.; Smith, D. R.; Mikkelsen, M. H. *Nat. Photonics* **2014**, *8*, 835.
(95) Kelly, C. V.; Wakefield, D. L.; Holowka, D. A.; Craighead, H. G.; Baird, B. A. *ACS Nano* **2014**, *8*, 7392.
(96) Lin, F.; Zhao, X.; Wang, J.; Yu, S.; Deng, Y.; Geng, L.; Li, H. *Analyst* **2014**, *139*, 2890.
(97) Wang, H.-S.; Wang, C.; He, Y.-K.; Xiao, F.-N.; Bao, W.-J.; Xia, X.-H.; Zhou, G.-J. *Anal. Chem.* **2014**, *86*, 3013.
(98) Acimovic, S. S.; Ortega, M. A.; Sanz, V.; Berthelot, J.; Garcia-Cordero, J. L.; Renger, J.; Maerkl, S. J.; Kreuzer, M. P.; Quidant, R. *Nano Lett.* **2014**, *14*, 2636.
(99) Lee, K. L.; You, M. L.; Tsai, C. H.; Lin, E. H.; Hsieh, S. Y.; Ho, M. H.; Hsu, J. C.; Wei, P. K. *Biosens. Bioelectron.* **2016**, *75*, 88.
(100) Betz, J. F.; Yu, W. W.; Cheng, Y.; White, I. M.; Rubloff, G. W. *Phys. Chem. Chem. Phys.* **2014**, *16*, 2224.
(101) Meier, T. A.; Poehler, E.; Kemper, F.; Pabst, O.; Jahnke, H. G.; Beckert, E.; Robitzki, A.; Belder, D. *Lab Chip* **2015**, *15*, 2923.
(102) Meier, T. A.; Beulig, R. J.; Klinge, E.; Fuss, M.; Ohla, S.; Belder, D. *Chem. Commun. (Cambridge, U. K.)* **2015**, *51*, 8588.
(103) Negri, P.; Flaherty, R. J.; Dada, O. O.; Schultz, Z. D. *Chem. Commun.* **2014**, *50*, 2707.
(104) Bailey, M. R.; Pentecost, A. M.; Selimovic, A.; Martin, R. S.; Schultz, Z. D. *Anal. Chem.* **2015**, *87*, 4347.
(105) Li, M.; Zhao, F.; Zeng, J.; Qi, J.; Lu, J.; Shih, W.-C. *J. Biomed. Opt.* **2014**, *19*, 111611.
(106) Qi, J.; Zeng, J.; Zhao, F.; Lin, S. H.; Raja, B.; Strych, U.; Willson, R. C.; Shih, W.-C. *Nanoscale* **2014**, *6*, 8521.
(107) Visaveliya, N.; Koehler, J. M. *Small* **2015**, DOI: 10.1002/smll.201502364.
(108) Black, W. A.; Stocks, B. B.; Mellors, J. S.; Engen, J. R.; Ramsey, J. M. *Anal. Chem.* **2015**, *87*, 6280.
(109) van den Brink, F. T. G.; Bueter, L.; Odijk, M.; Olthuis, W.; Karst, U.; van den Berg, A. *Anal. Chem.* **2015**, *87*, 1527.
(110) Wang, S.; Chen, S.; Wang, J.; Xu, P.; Luo, Y.; Nie, Z.; Du, W. *Electrophoresis* **2014**, *35*, 2528.

DOI: 10.1021/acs.analchem.5b04310
Anal. Chem. 2016, 88, 320−338

(111) Verboket, P. E.; Borovinskaya, O.; Meyer, N.; Guenther, D.; Dittrich, P. S. *Anal. Chem.* **2014**, *86*, 6012.
(112) Thacker, V. V.; Bromek, K.; Meijer, B.; Kotar, J.; Sclavi, B.; Lagomarsino, M. C.; Keyser, U. F.; Cicuta, P. *Integrative Biology* **2014**, *6*, 184.
(113) Guo, J.; Li, C. M.; Kang, Y. *Biomed. Microdevices* **2014**, *16*, 681.
(114) Jiang, J.; Wang, X.; Chao, R.; Ren, Y.; Hu, C.; Xu, Z.; Liu, G. L. *Sens. Actuators, B* **2014**, *193*, 653.
(115) Zhao, Y.; Zhao, X. T.; Chen, D. Y.; Luo, Y. N.; Jiang, M.; Wei, C.; Long, R.; Yue, W. T.; Wang, J. B.; Chen, J. *Biosens. Bioelectron.* **2014**, *57*, 245.
(116) Huck, C.; Poghossian, A.; Baecker, M.; Chaudhuri, S.; Zander, W.; Schubert, J.; Begoyan, V. K.; Buniatyan, V. V.; Wagner, P.; Schoening, M. J. *Sens. Actuators, B* **2014**, *198*, 102.
(117) Martinez-Cisneros, C. S.; Sanchez, S.; Xi, W.; Schmidt, O. G. *Nano Lett.* **2014**, *14*, 2219.
(118) Beuvier, T.; Panduro, E. A. C.; Kwasniewski, P.; Marre, S.; Lecoutre, C.; Garrabos, Y.; Aymonier, C.; Calvignac, B.; Gibaud, A. *Lab Chip* **2015**, *15*, 2002.
(119) Ryan, H.; Smith, A.; Utz, M. *Lab Chip* **2014**, *14*, 1678.
(120) Ghazani, A. A.; Pectasides, M.; Sharma, A.; Castro, C. M.; Mino-Kenudson, M.; Lee, H.; Shepard, J.-A. O.; Weissleder, R. *Nanomedicine* **2014**, *10*, 661.
(121) Bianco, V.; Paturzo, M.; Finizio, A.; Calabuig, A.; Javidi, B.; Ferraro, P. *IEEE J. Sel. Topics Quantum Electron.* **2014**, *20*, 6801507.
(122) Bianco, V.; Merola, F.; Miccio, L.; Memmolo, P.; Gennari, O.; Paturzo, M.; Netti, P. A.; Ferraro, P. *Lab Chip* **2014**, *14*, 2499.
(123) Bianco, V.; Paturzo, M.; Marchesano, V.; Gallotta, I.; Di Schiavi, E.; Ferraro, P. *Lab Chip* **2015**, *15*, 2117.
(124) Zhu, G.-P.; Hejiazan, M.; Huang, X.; Nguyen, N.-T. *Lab Chip* **2014**, *14*, 4609.
(125) Li, L.; Li, P.; Fang, J.; Li, Q.; Xiao, H.; Zhou, H.; Tang, B. *Anal. Chem.* **2015**, *87*, 6057.
(126) Bulbul, A.; Kim, H. *Lab Chip* **2015**, *15*, 94.
(127) Gerber, L. C.; Rosenfeld, L.; Chen, Y.; Tang, S. K. Y. *Lab Chip* **2014**, *14*, 4324.
(128) Leuthold, L. A.; Heudi, O.; Deglon, J.; Raccuglia, M.; Augsburger, M.; Picard, F.; Kretz, O.; Thomas, A. *Anal. Chem.* **2015**, *87*, 2068.
(129) Yang, J.; Nam, Y.-G.; Lee, S.-K.; Kim, C.-S.; Koo, Y.-M.; Chang, W.-J.; Gunasekaran, S. *Sens. Actuators, B* **2014**, *203*, 44.
(130) Hu, J.-B.; Chen, S.-Y.; Wu, J.-T.; Chen, Y.-C.; Urban, P. L. *RSC Adv.* **2014**, *4*, 10693.
(131) Kuester, S. K.; Pabst, M.; Jefimovs, K.; Zenobi, R.; Dittrich, P. S. *Anal. Chem.* **2014**, *86*, 4848.
(132) Hu, Z.; Glidle, A.; Ironside, C.; Cooper, J. M.; Yin, H. *Lab Chip* **2015**, *15*, 283.
(133) Rival, A.; Jary, D.; Delattre, C.; Fouillet, Y.; Castellan, G.; Bellemin-Comte, A.; Gidrol, X. *Lab Chip* **2014**, *14*, 3739.
(134) Shih, S. C. C.; Gach, P. C.; Sustarich, J.; Simmons, B. A.; Adams, P. D.; Singh, S.; Singh, A. K. *Lab Chip* **2015**, *15*, 225.
(135) He, J.-L.; Chen, A.-T.; Lee, J.-H.; Fan, S.-K. *Int. J. Mol. Sci.* **2015**, *16*, 22319.
(136) Kumar, P. T.; Toffalini, F.; Witters, D.; Vermeir, S.; Rolland, F.; Hertog, M. L. A. T. M.; Nicolai, B. M.; Puers, R.; Geeraerd, A.; Lammertyn, J. *Sens. Actuators, B* **2014**, *199*, 479.
(137) Ko, H.; Lee, J.; Kim, Y.; Lee, B.; Jung, C.-H.; Choi, J.-H.; Kwon, O.-S.; Shin, K. *Adv. Mater. (Weinheim, Ger.)* **2014**, *26*, 2335.
(138) Lafreniere, N. M.; Mudrik, J. M.; Ng, A. H. C.; Seale, B.; Spooner, N.; Wheeler, A. R. *Anal. Chem.* **2015**, *87*, 3902.
(139) Lafreniere, N. M.; Shih, S. C. C.; Abu-Rabie, P.; Jebrail, M. J.; Spooner, N.; Wheeler, A. R. *Bioanalysis* **2014**, *6*, 307.
(140) Zhu, Z.; Guan, Z.; Jia, S.; Lei, Z.; Lin, S.; Zhang, H.; Ma, Y.; Tian, Z.-Q.; Yang, C. J. *Angew. Chem., Int. Ed.* **2014**, *53*, 12503.
(141) Trantum, J. R.; Baglia, M. L.; Eagleton, Z. E.; Mernaugh, R. L.; Haselton, F. R. *Lab Chip* **2014**, *14*, 315.
(142) Nosrati, R.; Vollmer, M.; Eamer, L.; San Gabriel, M. C.; Zeidan, K.; Zini, A.; Sinton, D. *Lab Chip* **2014**, *14*, 1142.
(143) Yang, F.; Zuo, X.; Li, Z.; Deng, W.; Shi, J.; Zhang, G.; Huang, Q.; Song, S.; Fan, C. *Adv. Mater.* **2014**, *26*, 4671.
(144) Li, Y.; Xuan, J.; Xia, T.; Han, X.; Song, Y.; Cao, Z.; Jiang, X.; Guo, Y.; Wang, P.; Qin, L. *Anal. Chem.* **2015**, *87*, 3771.
(145) Li, B.; Li, L.; Guan, A.; Dong, Q.; Ruan, K.; Hu, R.; Li, Z. *Lab Chip* **2014**, *14*, 4085.
(146) Laksanasopin, T.; Guo, T. W.; Nayak, S.; Sridhara, A. A.; Xie, S.; Olowookere, O. O.; Cadinu, P.; Meng, F.; Chee, N. H.; Kim, J.; Chin, C. D.; Munyazesa, E.; Mugwaneza, P.; Rai, A. J.; Mugisha, V.; Castro, A. R.; Steinmiller, D.; Linder, V.; Justman, J. E.; Nsanzimana, S.; Sia, S. K. *Sci. Transl. Med.* **2015**, *7*, 273re1.
(147) Wang, S.; Tasoglu, S.; Chen, P. Z.; Chen, M.; Akbas, R.; Wach, S.; Ozdemir, C. I.; Gurkan, U. A.; Giguel, F. F.; Kuritzkes, D. R.; Demirci, U. *Sci. Rep.* **2014**, *4*, 3796.
(148) Merola, F.; Memmolo, P.; Miccio, L.; Bianco, V.; Paturzo, M.; Ferraro, P. *Proc. IEEE* **2015**, *103*, 192.
(149) Nguyen, J.; Wei, Y.; Zheng, Y.; Wang, C.; Sun, Y. *Lab Chip* **2015**, *15*, 1533.
(150) Novo, P.; Chu, V.; Conde, J. P. *Biosens. Bioelectron.* **2014**, *57*, 284.
(151) Son, J. H.; Lee, S. H.; Hong, S.; Park, S.-m.; Lee, J.; Dickey, A. M.; Lee, L. P. *Lab Chip* **2014**, *14*, 2287.
(152) Safavieh, M.; Ahmed, M. U.; Ng, A.; Zourob, M. *Biosens. Bioelectron.* **2014**, *58*, 101.
(153) Safavieh, M.; Ahmed, M. U.; Sokullu, E.; Ng, A.; Braescu, L.; Zourob, M. *Analyst* **2014**, *139*, 482.
(154) Koh, C.-Y.; Schaff, U. Y.; Piccini, M. E.; Stanker, L. H.; Cheng, L. W.; Ravichandran, E.; Singh, B.-R.; Sommer, G. J.; Singh, A. K. *Anal. Chem.* **2015**, *87*, 922.
(155) Schuler, F.; Schwemmer, F.; Trotter, M.; Wadle, S.; Zengerle, R.; von Stetten, F.; Paust, N. *Lab Chip* **2015**, *15*, 2759.
(156) Clime, L.; Brassard, D.; Geissler, M.; Veres, T. *Lab Chip* **2015**, *15*, 2400.
(157) Schwemmer, F.; Zehnle, S.; Mark, D.; von Stetten, F.; Zengerle, R.; Paust, N. *Lab Chip* **2015**, *15*, 1545.
(158) Aeinehvand, M. M.; Ibrahim, F.; Harun, S. W.; Al-Faqheri, W.; Thio, T. H. G.; Kazemzadeh, A.; Madou, M. *Lab Chip* **2014**, *14*, 988.
(159) Li, C. G.; Dangol, M.; Lee, C. Y.; Jang, M.; Jung, H. *Lab Chip* **2015**, *15*, 382.
(160) Baudoin, R.; Legendre, A.; Jacques, S.; Cotton, J.; Bois, F.; Leclerc, E. *J. Pharm. Sci.* **2014**, *103*, 706.
(161) Au, S. H.; Chamberlain, M. D.; Mahesh, S.; Sefton, M. V.; Wheeler, A. R. *Lab Chip* **2014**, *14*, 3290.
(162) Scanlon, T. C.; Dostal, S. M.; Griswold, K. E. *Biotechnol. Bioeng.* **2014**, *111*, 232.
(163) Caviglia, C.; Zor, K.; Montini, L.; Tilli, V.; Canepa, S.; Melander, F.; Muhammad, H. B.; Carminati, M.; Ferrari, G.; Raiteri, R.; Heiskanen, A.; Andresen, T. L.; Emneus, J. *Anal. Chem.* **2015**, *87*, 2204.
(164) Akagi, J.; Zhu, F.; Hall, C. J.; Crosier, K. E.; Crosier, P. S.; Wlodkowic, D. *Cytometry, Part A* **2014**, *85*, 537.
(165) Weltin, A.; Slotwinski, K.; Kieninger, J.; Moser, I.; Jobst, G.; Wego, M.; Ehret, R.; Urban, G. A. *Lab Chip* **2014**, *14*, 138.
(166) Czilwik, G.; Schwarz, I.; Keller, M.; Wadle, S.; Zehnle, S.; von Stetten, F.; Mark, D.; Zengerle, R.; Paust, N. *Lab Chip* **2015**, *15*, 1084.
(167) Gan, W.; Zhuang, B.; Zhang, P.; Han, J.; Li, C.-X.; Liu, P. *Lab Chip* **2014**, *14*, 3719.
(168) Warkiani, M. E.; Tay, A. K. P.; Khoo, B. L.; Xu, X.; Han, J.; Lim, C. T. *Lab Chip* **2015**, *15*, 1101.
(169) Zhang, R.; Li, X.; Ramaswami, G.; Smith, K. S.; Turecki, G.; Montgomery, S. B.; Li, J. B. *Nat. Methods* **2014**, *11*, 51.
(170) Zhu, Q.; Qiu, L.; Yu, B.; Xu, Y.; Gao, Y.; Pan, T.; Tian, Q.; Song, Q.; Jin, W.; Jin, Q.; Mu, Y. *Lab Chip* **2014**, *14*, 1176.
(171) Eastburn, D. J.; Sciambi, A.; Abate, A. R. *Nucleic Acids Res.* 2014, *42*.
(172) Lin, X.; Chen, Q.; Liu, W.; Li, H.; Lin, J.-M. *Biosens. Bioelectron.* **2014**, *56*, 71.
(173) Reinholt, S. J.; Behrent, A.; Greene, C.; Kalfe, A.; Baeumner, A. J. *Anal. Chem.* **2014**, *86*, 849.

DOI: 10.1021/acs.analchem.5b04310
Anal. Chem. 2016, 88, 320−338

(174) Kersting, S.; Rausch, V.; Bier, F. F.; von Nickisch-Rosenegk, M. *Microchim. Acta* **2014**, *181*, 1715.
(175) Lee, J.-J.; Jeong, K. J.; Hashimoto, M.; Kwon, A. H.; Rwei, A.; Shankarappa, S. A.; Tsui, J. H.; Kohane, D. S. *Nano Lett.* **2014**, *14*, 1.
(176) Shao, N.; Jiang, S.-M.; Zhang, M.; Wang, J.; Guo, S.-J.; Li, Y.; Jiang, H.-W.; Liu, C.-X.; Zhang, D.-B.; Yang, L.-T.; Tao, S.-C. *Anal. Chem.* **2014**, *86*, 1269.
(177) Su, Y.-C.; Wang, C.-H.; Chang, W.-H.; Chen, T.-Y.; Lee, G.-B. *Biosens. Bioelectron.* **2015**, *63*, 196.
(178) Zhang, Y.; Sun, J.; Zou, Y.; Chen, W.; Zhang, W.; Xi, J. J.; Jiang, X. *Anal. Chem.* **2015**, *87*, 900.
(179) Luo, X.; Tsao, C. Y.; Wu, H. C.; Quan, D. N.; Payne, G. F.; Rubloff, G. W.; Bentley, W. E. *Lab Chip* **2015**, *15*, 1842.
(180) Ma, L.; Kim, J.; Hatzenpichler, R.; Karymov, M. A.; Hubert, N.; Hanan, I. M.; Chang, E. B.; Ismagilov, R. F. *Proc. Natl. Acad. Sci. U. S. A.* **2014**, *111*, 9768.
(181) Yawata, Y.; Cordero, O. X.; Menolascina, F.; Hehemann, J.-H.; Polz, M. F.; Stocker, R. *Proc. Natl. Acad. Sci. U. S. A.* **2014**, *111*, 5622.
(182) Song, W.; Fadaei, H.; Sinton, D. *Environ. Sci. Technol.* **2014**, *48*, 3567.
(183) Cogan, D.; Fay, C.; Boyle, D.; Osborne, C.; Kent, N.; Cleary, J.; Diamond, D. *Anal. Methods* **2015**, *7*, 5396.
(184) Foan, L.; Ricoul, F.; Vignoud, S. *Int. J. Environ. Anal. Chem.* **2015**, *95*, 1171.
(185) Korir, G.; Prakash, M. *PLoS One* **2015**, *10*, e0115993.
(186) Long, F.; Wang, H.; Zhu, A. *Anal. Chim. Acta* **2014**, *849*, 43.
(187) Golberg, A.; Linshiz, G.; Kravets, I.; Stawski, N.; Hillson, N. J.; Yarmush, M. L.; Marks, R. S.; Konry, T. *PLoS One* **2014**, *9*, e86341.
(188) Harrison, H.; Lu, X.; Patel, S.; Thomas, C.; Todd, A.; Johnson, M.; Raval, Y.; Tzeng, T.-R.; Song, Y.; Wang, J.; Li, D.; Xuan, X. *Analyst (Cambridge, U. K.)* **2015**, *140*, 2869.
(189) Ishii, S.; Nakamura, T.; Ozawa, S.; Kobayashi, A.; Sano, D.; Okabe, S. *Environ. Sci. Technol.* **2014**, *48*, 4744.
(190) Ishikawa, T.; Shioiri, T.; Numayama-Tsuruta, K.; Ueno, H.; Imai, Y.; Yamaguchi, T. *Lab Chip* **2014**, *14*, 1023.
(191) Sackmann, E. K.-H.; Berthier, E.; Schwantes, E. A.; Fichtinger, P. S.; Evans, M. D.; Dziadzio, L. L.; Huttenlocher, A.; Mathur, S. K.; Beebe, D. J. *Proc. Natl. Acad. Sci. U. S. A.* **2014**, *111*, 5813.
(192) Sahari, A.; Traore, M. A.; Scharf, B. E.; Behkam, B. *Biomed. Microdevices* **2014**, *16*, 717.
(193) Dey, K. K.; Das, S.; Poyton, M. F.; Sengupta, S.; Butler, P. J.; Cremer, P. S.; Sen, A. *ACS Nano* **2014**, *8*, 11941.
(194) Araci, I. E.; Su, B.; Quake, S. R.; Mandel, Y. *Nat. Med.* **2014**, *20*, 1074.
(195) Cable, M. L.; Hoerst, S. M.; He, C.; Stockton, A. M.; Mora, M. F.; Tolbert, M. A.; Smith, M. A.; Willis, P. A. *Earth Planet. Sci. Lett.* **2014**, *403*, 99.
(196) Mok, J.; Mindrinos, M. N.; Davis, R. W.; Javanmard, M. *Proc. Natl. Acad. Sci. U. S. A.* **2014**, *111*, 2110.

DOI: 10.1021/acs.analchem.5b04310
Anal. Chem. 2016, 88, 320−338